Electronic Supplementary Material (ESI) for ChemComm.
This journal is © The Royal Society of Chemistry 2024

Supplementary Information

Columnar liquid crystals based on antiaromatic expanded porphyrins.

Duong D. Nguyen,[a] Jorge Labella,*[b] Juan Laforga-Martín,[b] César L. Folcia,[c] Josu Ortega,[c] Tomás Torres,*[b,d,e] Teresa Sierra*[f] and Jonathan L. Sessler. *[a]

[a.] Department of Chemistry, The University of Texas at Austin, 105 E 24th Street A5300, Austin, TX, 78712, United States. E-mail: sessler@cm.utexas.edu
[b.] Department of Organic Chemistry, Universidad Autónoma de Madrid, Campus de Cantoblanco, C/ Francisco Tomás y Valiente 7, 28049 Madrid (Spain)
E-mail: jorge.labella; tomas.torres@uam.es
[c.] Department of Physics, Faculty of Science and Technology, UPV/EHU, Bilbao, Spain
[d.] Institute for Advanced Research in Chemical Sciences (IAdChem), Universidad Autónoma de Madrid, 28049 Madrid, Spain
[e.] IMDEA-Nanociencia, Campus de Cantoblanco, 28049 Madrid, Spain
[f.] Instituto de Nanociencia y Materiales de Aragón (INMA), Departamento de Química Orgánica, Facultad de Ciencias, CSIC-Universidad de Zaragoza, 50009 Zaragoza, Spain.

1. Instrumentation and materials

Reaction progress was monitored by thin layer chromatography (TLC), employing aluminum sheets coated with silica gel type 60 F254 (0.2 mm thick, Merck) and a 254 and 365 nm UV lamp. Purification and separation of the synthesized products was performed by normal-phase column chromatography, using silica gel (230–400 mesh, 0.040–0.063 mm, Merck) and size exclusion chromatography, using Bio-Beads^{TM} S-X1 (styrene divinylbenzene beads, 40-80 μm bead size, Bio-Rad). Eluents along with the relative ratio in the case of solvent mixtures are indicated for each particular case. Nuclear magnetic resonance spectra (^{1}H-, ^{13}C-,^{11}B-, ^{19}F-NMR) were recorded on Agilent MR400, Bruker AV-400, Bruker DRX-500 or Varian MR600 spectrometers at the Department of Chemistry of The University of Texas at Austin. The deuterated solvent employed in each case is indicated in brackets, and its residual peak was used to calibrate the spectra using literature reference δ ppm values.[1] The peaks marked with asterisks indicates solvent residue signals. The NMR spectroscopic solvents were purchased from Cambridge Isotope Laboratories and Fischer Scientific. All spectra were recorded at room temperature. High resolution ESI mass spectrometry was carried out using an Ion Spec Fourier Transform mass spectrometer (9.4 T). Electrospray ionization (ESI) mass spectra were recorded on an Agilent Technologies 6530 Accurate-Mass Q-TOF instrument housed in the Department of Chemistry of The University of Texas at Austin. Matrix-assisted laser desorption/ionization (MALDI) mass spectra were recorded using a Bruker AutoFLEX III-TOF/TOF spectrometer and DCTB as matrix. These measurements (accuracy= 50 ppm) were conducted using external calibration. The matrixes and internal references employed are indicated for each spectrum. Ultraviolet-visible (UV-Vis) spectra were recorded using spectroscopic grade solvents using a Varian Cary 5000 spectrophotometer housed in the in the Department of Chemistry of The University of Texas at Austin. The logarithm of the molar extinction coefficient (ε) is indicated in brackets for each maximum. Chemicals were purchased from commercial suppliers and used without further purification. Dry solvents were purchased from commercial suppliers as anhydrous grade or thoroughly dried before use employing standard methods. Solid, hygroscopic reagents were dried in a vacuum oven before use. The synthesis and characterization of naphthobipyrrole has been previously reported.[2]

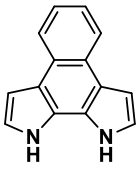

Naphthobipyrrole

Liquid crystal behavior was examined by polarizing optical microscopy using a polarizing optical microscope Olympus BX51 equipped with an Olympus DP152 digital camera and connected to a Linkam THMS600 hot stage and a Linkam TMS94 controller. Transition temperatures and enthalpies were obtained by differential scanning calorimetry with DSC TA instruments Q20 and Q2000 at heating and cooling rates of 10 °C min^{-1}. X-ray diffraction diagrams were recorded using a Stoe Stadivari goniometer equipped with a Genix3D microfocus generator (Xenocs) and a Dectris Pilatus 100K detector. Temperature control was achieved using a nitrogen-gas Cryostream controller (Oxford Cryosystems) allowing for a temperature control of about 0.1 ºC. Lindemann capillaries of diameter 0.6 mm were utilized. Monochromatic Cu-Kα radiation (λ = 1.5418 Å) was used.

2. Synthetic Procedures and Compound Data

Synthesis and characterization of aldehyde precursors

4-(3-Bromopropoxy)-2,6-difluorobenaldehyde

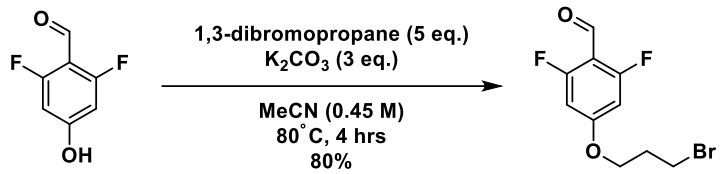

To a 100 mL round-bottomed flask containing 4-hydroxy-2,6-difluorobenzaldehyde (3 g, 19 mmol) and K_2CO_3 (7.87 g, 57 mmol, 3 equiv.) dissolved in acetonitrile (40 mL), was added 1,3-dibromopropane (9.7 mL, 95 mmol, 5 equiv.). The mixture was then stirred at 80°C for 4 hours. Upon completion, the reaction mixture was concentrated in vacuo. Dichloromethane (100 mL) was added, then the solution was washed with brine (100 mL) and water (100 mL). The solution was dried over Na_2SO_4, and the volatiles were fully evaporated off. The crude mixture was purified via silica gel column chromatography using hexanes: ethyl acetate = 6:1 as the eluent. **Yield** 4.5 g, 85% yield, white crystalline solid. **^{1}H NMR** (500 MHz, $CDCl_3$) δ (ppm) = 10.20 (s, 1H), 6.51 (d, *J* = 10.5 Hz, 2H), 4.17 (t, *J* = 5.8 Hz, 2H), 3.58 (t, *J* = 6.2 Hz, 2H), 2.35 (p, *J* = 6.1 Hz, 2H). **^{13}C NMR** (126 MHz, $CDCl_3$): δ (ppm) = 160.19 (t, J_{CF} = 4.3 Hz), 142.50 (d, J_{CF} = 9.1 Hz), 141.66 (t, J_{CF} = 15.1 Hz), 140.42 (d, J_{CF} = 9.1 Hz), 85.18 (t, J_{CF} = 11.2 Hz), 75.94 (d, J_{CF} = 27.8 Hz), 43.39, 8.44, 5.90. **^{19}F NMR** (417 MHz, $CDCl_3$) δ (ppm) = -112.74 (d, *J* = 11.2 Hz). **HRMS** (ESI positive): *m/z* [M+Na^+] Calculated for $C_{10}H_9BrF_2O_2$: 300.9646, found: 300.9655.

4-(3-Bromopropoxy)-3,5-difluorobenaldehyde

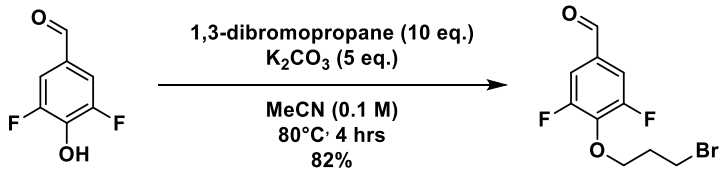

To a 100 mL round-bottomed flask containing 4-hydroxy-2,6-difluorobenzaldehyde (3 g, 19 mmol) and K_2CO_3 (7.87 g, 57 mmol, 3 equiv.) dissolved in acetonitrile (40 mL) was added 1,3-dibromopropane (9.7 mL, 95 mmol, 5 equiv.). The mixture was stirred at 80°C for 4 hours. When the reaction was deemed complete, the reaction mixture was concentrated in vacuo. Dichloromethane (100 mL) was added, then the solution was washed with brine (100 mL) and water (100 mL). The solution was dried over Na_2SO_4, and the volatiles were fully evaporated off. The crude mixture was purified via silica gel column chromatography using hexanes: ethyl acetate = 6:1 to 4:1 gradient as the eluent. **Yield** 4.3 g, 82% yield, yellow oil. **^{1}H NMR** (500 MHz, $CDCl_3$): δ (ppm) = 9.84 (s, 1H), 7.45 (d, *J* = 8.4 Hz, 2H), 4.43 (t, *J* = 5.8 Hz, 2H), 3.64 (t, *J* = 6.4 Hz, 2H), 2.31 (p, *J* = 6.0 Hz, 2H). **^{13}C NMR** (126 MHz, $CDCl_3$): δ (ppm) = 165.54 (t, *J* = 2.3 Hz), 132.42 (dd, *J* = 251.9, 5.4 Hz), 117.73 (t, *J* = 13.8 Hz), 107.51 (t, *J* = 6.7 Hz), 90.24 (dd), 48.81, 9.75, 6.02. **^{19}F NMR** (471 MHz, $CDCl_3$): δ (ppm) = -125.75 (d, *J* = 7.2 Hz). **HRMS** (ESI positive): *m/z* [M+H^+] Calculated for $C_{10}H_9BrF_2O_2$: 278.9827, found: 278.9829.

3,5-Bis(3-bromopropoxy)-2,6-difluorobenaldehyde

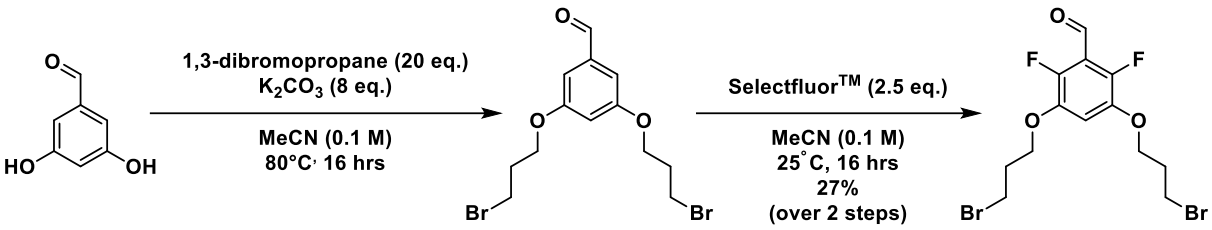

Step 1: To a 100 mL round-bottomed flask containing 3,5-dihydroxybenzaldehyde (2 g, 14.48 mmol) and K_2CO_3 10.1 g, 72 mmol, 5 equiv.) dissolved in acetonitrile (48 mL) was added 1,3-dibromopropane (14.76 mL, 145 mmol, 10 equiv.). The mixture was then stirred at 80°C for 20 hours. Once deemed complete, the reaction mixture was concentrated in vacuo. Dichloromethane (100 mL) was added, then the solution was washed with brine (100 mL) and water (100 mL). The solution was dried over Na_2SO_4, and the volatiles fully evaporated off. The crude product obtained in this way was subjected to the next step without any further purification.

Step 2: Using an ice bath, a solution of crude 3,5-bis(3-bromopropoxy)benzaldehyde in acetonitrile (15 mL) was cooled to 0°C. To the solution, SelectFluor^{TM} (7.7 g, 11 mmol, 1.5 equiv.) was added portion-wise while the temperature was kept below 0°C. The resulting mixture was stirred at 15°C for 16 hours. The reaction mixture was concentrated to remove solvent. The residue was diluted with water (10 mL) and neutralized with saturated $NaHCO_3$ solution. The product was extracted with ethyl acetate (10 mL x3). The collected fraction was then washed with brine (10 mL) and water (10 mL) before being dried over Na_2SO_4 and concentrated *in vacuo*. The resulting crude product was purified via silica gel column chromatography using hexanes: ethyl acetate = 4:1 as the eluent. **Yield** 1.5g, 27% (over two steps), off-white crystalline powder. **^{1}H NMR** (400 MHz, $CDCl_3$) δ (ppm) = 10.35 (s, 1H), 6.97 (td, *J* = 8.0, 1.8 Hz, 1H), 4.20 (td, *J* = 5.8, 1.8 Hz, 4H), 3.64 (td, *J* = 6.3, 1.9 Hz, 4H), 2.33 (dt, *J* = 6.0, 2.9 Hz, 4H). **^{13}C NMR** (101 MHz, $CDCl_3$) δ (ppm) = 184.88, 148.50, 145.99, 143.21, 110.46, 77.48, 77.16, 76.84, 68.60, 32.33, 29.71. **^{19}F NMR** (160.5 MHz, $CDCl_3$): δ (ppm) = -145.84 (dd, *J* = 8.1, 2.5 Hz). **HRMS** (ESI positive): *m/z* [M+Na^+] Calculated for $C_{13}H_{14}Br_2F_2O_3$: 436.9170, found: 436.9189.

Synthesis and characterization of naphthorosarin macrocycles

General procedure for the synthesis of naphthorosarin macrocycles

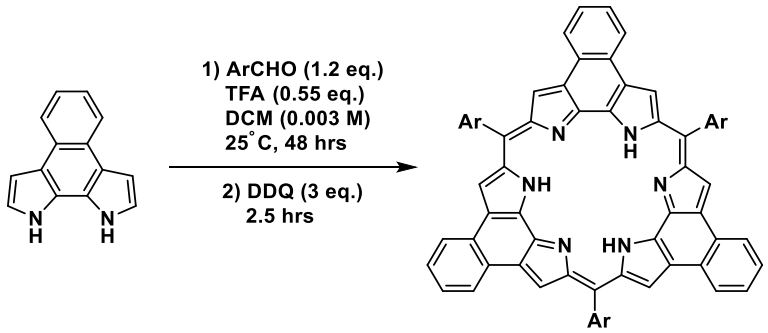

A 1 L round-bottomed flask was charged with naphthobipyrrole (100 mg, 0.484 mmol, 1 equiv.) and aldehyde (1.2 equiv.). Then dry dichloromethane (300 mL, 0.0015 M) was added to dissolve the solids. The reaction mixture was bubbled with nitrogen for 15 minutes and the flask fully covered with aluminum foil. Trifluoroacetic acid (20 μL, 0.26 mmol, 0.55 equiv.) was then slowly added via syringe. The reaction mixture was kept stirring at room temperature for 72 hours under nitrogen atmosphere. After this time, DDQ (352 mg, 1.55 mmol, 3.2 equiv.)

was added, and the reaction mixture was stirred for a further 90 minutes open to air and light. Once the reaction was deemed complete, excess triethylamine (0.5 mL) was added to the reaction flask and the whole solution was passed through a plug of neutral alumina. Excess dichloromethane (about 200 mL) was used to elute fully the dark purple fraction. The resulting obtained was then evaporated to dryness. The crude product was purified via silica gel column chromatography (doped with 1% triethylamine) to obtain the desired solid. Detailed column conditions are given below for each particular rosarin compounds. Finally, recrystallization of the solid from dichloromethane/methanol yielded naphthorosarin as a dark brown solid.

NRos-4

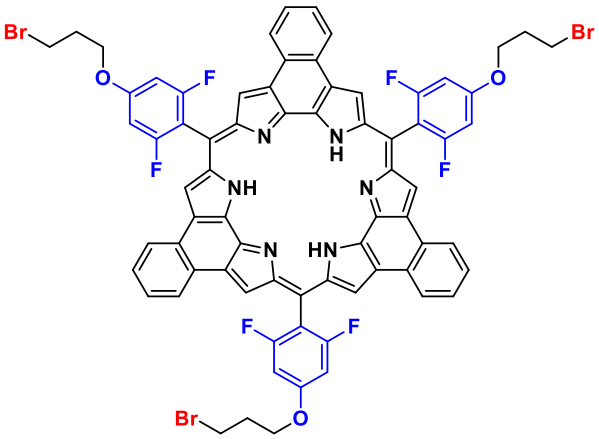

A 1 L round bottomed flask charged with naphthobipyrrole (100 mg, 0.484 mmol, 1 equiv.) and 4-(3-bromopropoxy)-2,6-difluorobenaldehyde (163 mg, 0.58 mmol, 1.2 equiv.). The general procedure was then followed to obtain a crude product. This crude product was purified via silica gel column chromatography (doped with 1% triethylamine) using dichloromethane: hexanes = 3:1 to 4:1 gradient. Finally, recrystallization of the solid from dichloromethane/methanol yielded **NRos-4** as a dark brown solid. **Yield** 33.8 mg, 15%. **^{1}H NMR** (600 MHz, TCE-d_2): δ (ppm) = 6.88 (br s, 12H), 6.67 (br s, 6H), 4.96 (s, 6H), 4.02 (t, J = 5.8 Hz, 6H), 3.53 (t, J = 6.3 Hz, 6H), 2.24 (p, J = 6.0 Hz, 6H). **^{13}C NMR** (151 MHz, TCE-d_2): δ (ppm) = 159.09, 158.07, 157.39, 149.04, 146.92, 129.96, 128.62, 123.74, 120.99, 120.84, 117.49, 96.77, 63.71, 29.52, 27.72. **^{19}F NMR** (564 MHz, TCE-d_2): δ (ppm) = -108.42. **HRMS** (ESI positive): m/z [M+H$^+$] Calculated for $C_{72}H_{45}Br_3F_6N_6O_3$: 1393.1080, found: 1393.1063. **UV-Vis** (DCM): λ_{max} (nm) (log ε(dm^3 cm^{-1} mol^{-1})): 475 (4.8), 582 (4.5)

NRos-5

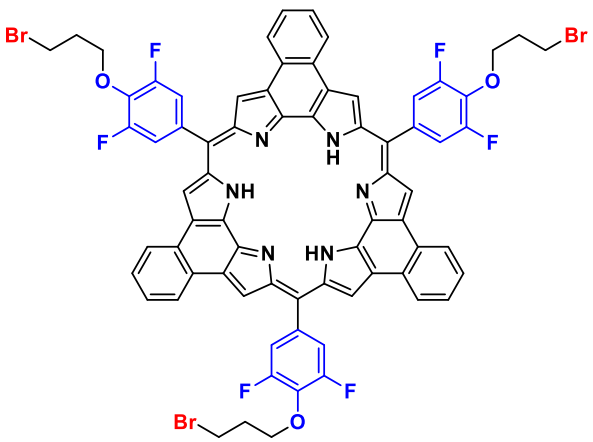

A 1 L round bottomed flask was charged with naphthobipyrrole (100 mg, 0.484 mmol, 1 equiv.) and 4-(3-bromopropoxy)-3,5-difluorobenaldehyde (163 mg, 0.58 mmol, 1.2 equiv.). The general procedure was then followed to obtain a crude product. This crude product was purified via silica gel column chromatography (doped with 1% triethylamine) using a dichloromethane: hexanes = 1:1 to 2:1 gradient as the eluent. Finally, recrystallization of the solid obtained after removal of the volatiles from dichloromethane/methanol yielded **NRos-5** as a dark brown solid. **Yield** 27.1 mg, 12%. **^{1}H NMR** (600 MHz, THF-d_8): δ (ppm) = 7.05 (s, 6H), 6.97 – 6.87 (m, 6H), 6.75 – 6.64 (m, 6H), 5.22 (s, 6H), 4.24 (t, *J* = 5.9 Hz, 6H), 3.62 (t, *J* = 6.5 Hz, 6H), 2.24 (p, *J* = 6.2 Hz, 6H).**^{13}C NMR** (151 MHz, THF-d_8): δ (ppm) = 157.60, 155.89, 151.17, 143.41, 132.21, 131.58, 126.99, 125.15, 124.36, 121.92, 113.79, 113.67, 73.18, 34.27, 30.32. **^{19}F NMR** (564 MHz, THF-d_8): δ (ppm) = -128.42 (d, *J* = 8.5 Hz). **HRMS** (ESI positive): *m/z* [M+H$^+$] Calculated for $C_{72}H_{45}Br_3F_6N_6O_3$: 1393.1080, found: 1393.1151. **UV-Vis** (DCM): λ_{max} (nm) (log ε(dm^3 cm^{-1} mol^{-1})): 482 (4.9), 573 (4.6).

NRos-6

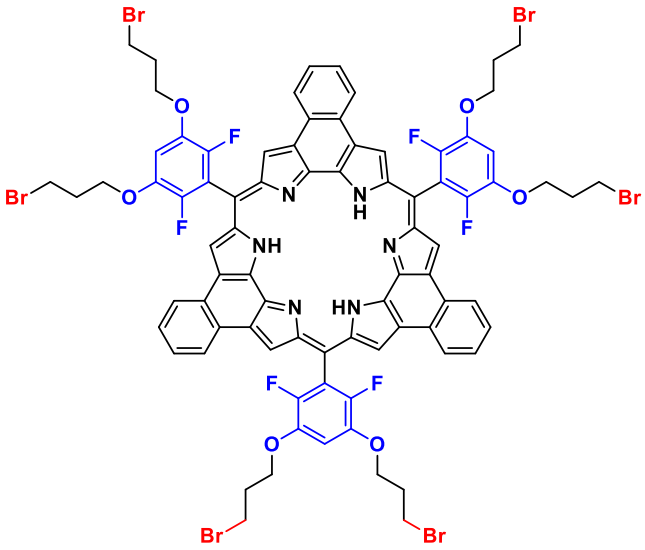

A 1 L round bottomed flask was charged with naphthobipyrrole (100 mg, 0.484 mmol, 1 equiv.) and 3,5-bis(3-bromopropoxy)-2,6-difluorobenaldehyde (242 mg, 0.58 mmol, 1.2 equiv.). The general procedure was then followed to obtain a crude product. This crude product was purified via silica gel column chromatography (doped with 1% triethylamine) using dichloromethane: hexanes = 1.5:1 as the eluent. Finally, recrystallization of the solid from dichloromethane/methanol yielded **NRos-6** as a dark brown solid. **Yield** 29.2 mg, 10%. **^{1}H NMR** (600 MHz, THF-d_8): δ (ppm) = 7.04 (dd, *J* = 5.9, 3.4 Hz, 6H), 6.93 (dd, *J* = 6.0, 3.4 Hz, 6H), 6.85 (t, *J* = 8.0 Hz, 3H), 5.07 (s, 6H), 4.11 (t, *J* = 5.9 Hz, 12H), 3.62 (t, *J* = 6.5 Hz, 12H), 2.27 (p, *J* = 6.2 Hz, 12H). **^{13}C NMR** (151 MHz, THF-d_8): δ (ppm) = 151.38, 145.09, 144.17, 144.09, 143.47, 133.02, 132.13, 126.86, 124.96, 124.46, 120.58, 105.05, 68.97, 33.61, 30.76. **^{19}F NMR** (564 MHz, THF-d_8): δ (ppm) = -141.55 (d, *J* = 8.0 Hz). **HRMS** (ESI positive): *m/z* [M+H$^+$] Calculated for $C_{81}H_{60}Br_6F_6N_6O_6$: 1800.9652, found: 1800.9748. **UV-Vis** (DCM): λ_{max} (nm) (log ε(dm^3 cm^{-1} mol^{-1})): 479 (5.0), 583 (4.7).

Synthesis and characterization of naphthorosarin macrocycles with alkyl chains

General synthetic scheme

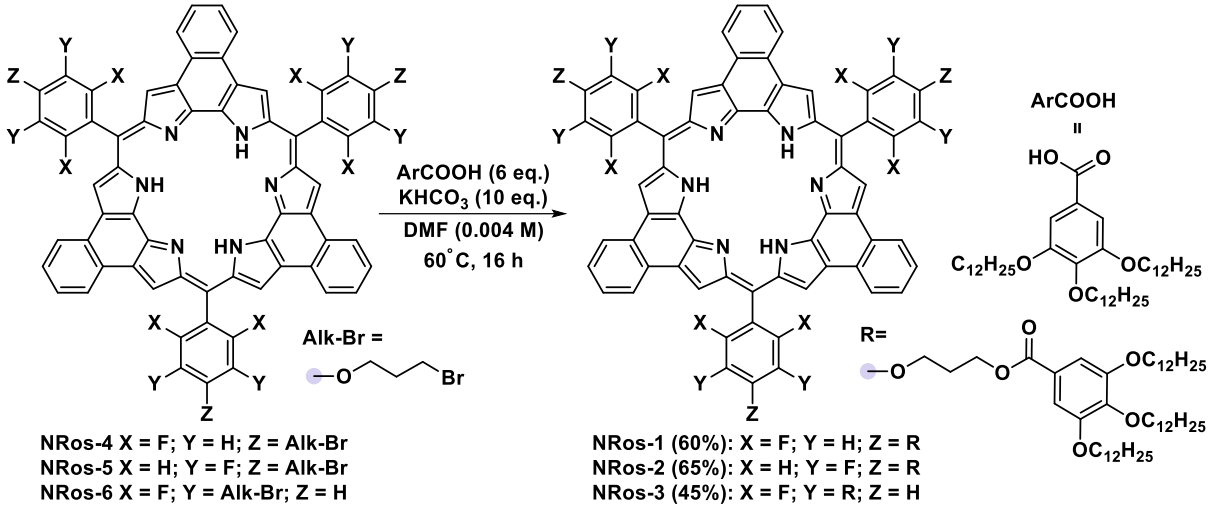

NRos-1

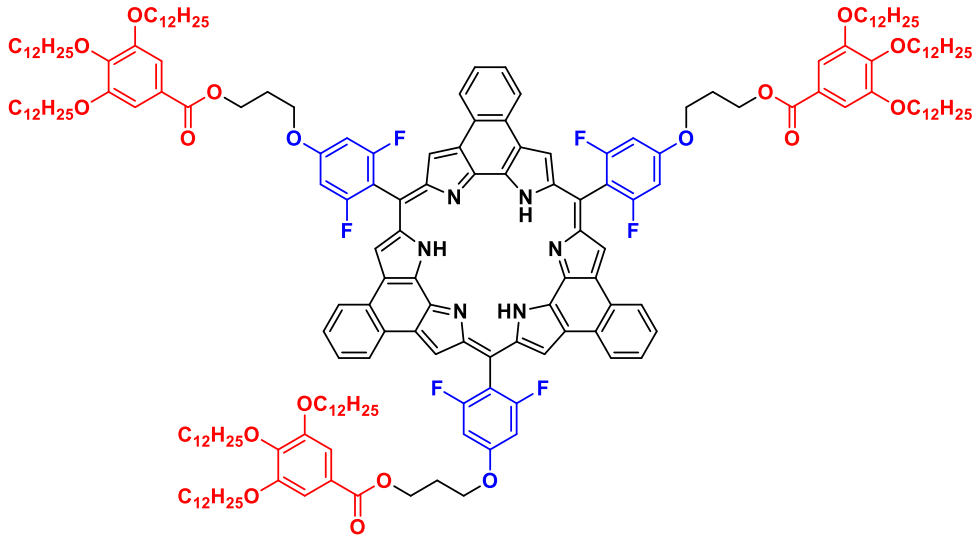

A 10 mL vial was charged with **NRos-4** (10 mg, 7.16 µmol, 1 equiv.), 3,4,5-tris(dodecyloxy)benzoic acid (29.02 mg, 42.98 µmol, 6 equiv.), and $KHCO_3$ (7.17 mg, 71.64 µmol, 10 equiv.) Then dry DMF (2 mL, 0.004 M) was added to dissolve the solids. The reaction mixture was stirred at 60°C for 16 hours. Hexanes (30 mL) were added, and the reaction mixture was washed with brine (20 mL x 3), water (20 mL), and DMF. The collected organic fraction was dried over Na_2SO_4, and the volatiles fully evaporated off. The resulting crude product was purified via silica gel column chromatography using a gradient of hexanes: ethyl acetate = 8:1 to 6/1 as the eluent. Finally, the product was further purified via size exclusion chromatography (Bio-Beads™ S-X1) using dichloromethane as the eluent to yield, after taking to dryness, the pure compound as a dark purple oily solid. **Yield** 13.66 mg, 60%. **^{1}H NMR** (600 MHz, THF-d_8): δ (ppm) = 7.23 (s, 6H), 7.08 (dd, J = 6.0, 3.4 Hz, 6H), 6.92 (dt, J = 7.5, 3.7 Hz, 6H), 6.60 (d, J = 9.7 Hz, 6H), 5.18 (s, 6H), 4.39 (t, J = 6.3 Hz, 6H), 4.11 (t, J = 6.2 Hz, 6H), 3.99 – 3.94 (m, 18H), 2.19 (p, J = 6.8 Hz, 6H), 1.77 (dd, J = 9.0, 6.2 Hz, 12H), 1.71 – 1.67 (m, 6H), 1.52 – 1.49 (m, 18H), 1.36 – 1.29 (m, 144H), 0.91 (d, J = 7.6 Hz, 27H). **^{13}C NMR** (151 MHz, THF-d_8): δ (ppm) = 166.50, 162.66, 162.05, 161.02, 154.07, 151.47, 143.96, 133.56, 131.77, 126.76, 125.83, 125.00, 124.38, 120.65, 109.10, 105.51, 99.75, 73.92, 70.05, 66.64, 62.34, 33.15, 33.11,

33.08, 33.06, 31.52, 30.92, 30.90, 30.88, 30.86, 30.84, 30.72, 30.60, 30.58, 30.54, 29.67, 27.28, 27.27, 25.95, 25.82, 23.79, 23.76, 14.67, 14.64. **^{19}F NMR** (564 MHz, THF-d_8): δ (ppm) = -111.92. **UV-Vis** (DCM): λ_{max} (nm) (log ε(dm^3 cm^{-1} mol^{-1})): 481 (5.1), 580 (4.9). MS (MALDI-TOF, DCTB): m/z [M+H^+] Calculated for $C_{201}H_{276}F_6N_6O_{18}$: 3177.1, found: 3176.7.

NRos-2

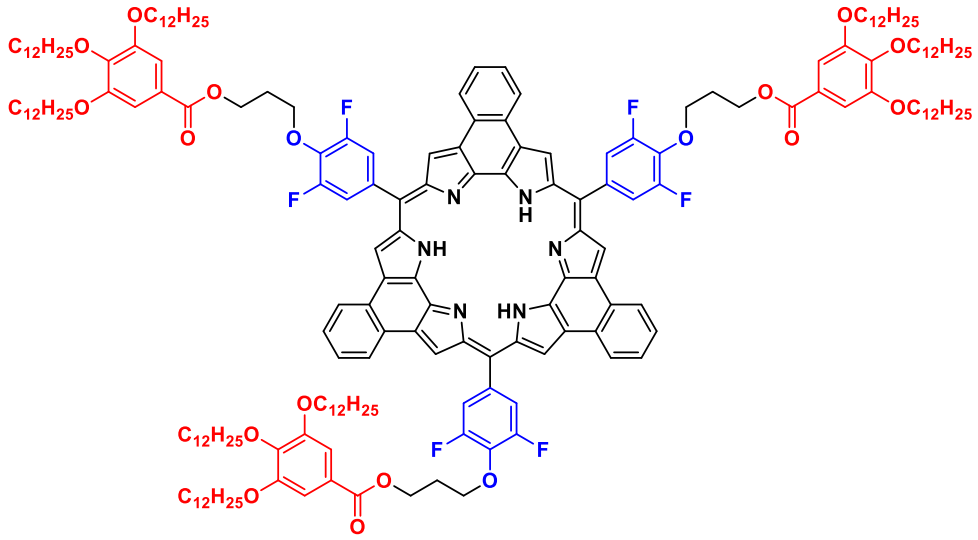

A 10 mL vial was charged with **NRos-5** (10 mg, 7.16 µmol, 1 equiv.), 3,4,5-tris(dodecyloxy)benzoic acid (29.02 mg, 42.98 µmol, 6 equiv.) and $KHCO_3$ (7.17 mg, 71.64 µmol, 10 equiv.). Then dry DMF (2 mL, 0.004 M) was added to dissolve the solids. The reaction mixture was stirred at 60°C for 16 hours. Hexanes (30 mL) were added, and the reaction mixture was washed with brine (20 mL x 3), water (20 mL), and DMF. The collected organic fraction was dried over Na_2SO_4, and the volatiles fully evaporated off. The crude product was purified via silica gel column chromatography using a gradient of hexanes: ethyl acetate = 8:1 to 6/1 as the eluent. Finally, the product was further purified via size exclusion chromatography (Bio-Beads^{TM} S-X1) using dichloromethane as an eluent to obtain, after drying, the title compound as a dark purple oily solid. **Yield** 14.79 mg, 65%. **^{1}H-NMR** (600 MHz, THF-d_8): 7.23 (s, 6H), 7.05 – 6.79 (m, 12H), 6.59 (s, 6H), 5.25 (s, 6H), 4.41 (t, *J* = 6.5 Hz, 6H), 4.27 (t, *J* = 6.1 Hz, 6H), 3.98 (t, *J* = 6.4 Hz, 9H), 3.94 (t, *J* = 6.3 Hz, 9H), 2.16 (h, *J* = 6.6 Hz, 6H), 1.79 (dd, *J* = 9.0, 6.2 Hz, 12H), 1.70 (d, *J* = 6.3 Hz, 6H), 1.54 – 1.49 (m, 18H), 1.38 – 1.28 (m, 144H), 0.90 (dp, *J* = 8.8, 4.3 Hz, 27H). **^{13}C-NMR** (151 MHz, THF-d_8): δ (ppm) = 166.48, 157.39, 155.74, 154.08, 154.04, 150.64, 143.84, 137.10, 132.06, 131.72, 126.76, 125.84, 125.22, 124.33, 121.90, 113.91, 109.00, 73.91, 72.11, 69.97, 62.12, 33.12, 33.08, 31.55, 30.95, 30.92, 30.90, 30.85, 30.83, 30.79, 30.75, 30.72, 30.65, 30.61, 30.59, 30.54, 30.49, 27.33, 27.29, 23.79, 23.76, 23.73, 14.67, 14.64. **^{19}F-NMR** (564 MHz, THF-d_8): δ (ppm) = -128.38. **UV-Vis** (DCM): λ_{max} (nm) (log ε(dm^3 cm^{-1} mol^{-1})): 489 (5.0), 580 (4.8). MS (MALDI-TOF, DCTB): m/z [M+H^+] Calculated for $C_{201}H_{276}F_6N_6O_{18}$: 3177.1, found: 3176.8.

NRos-3

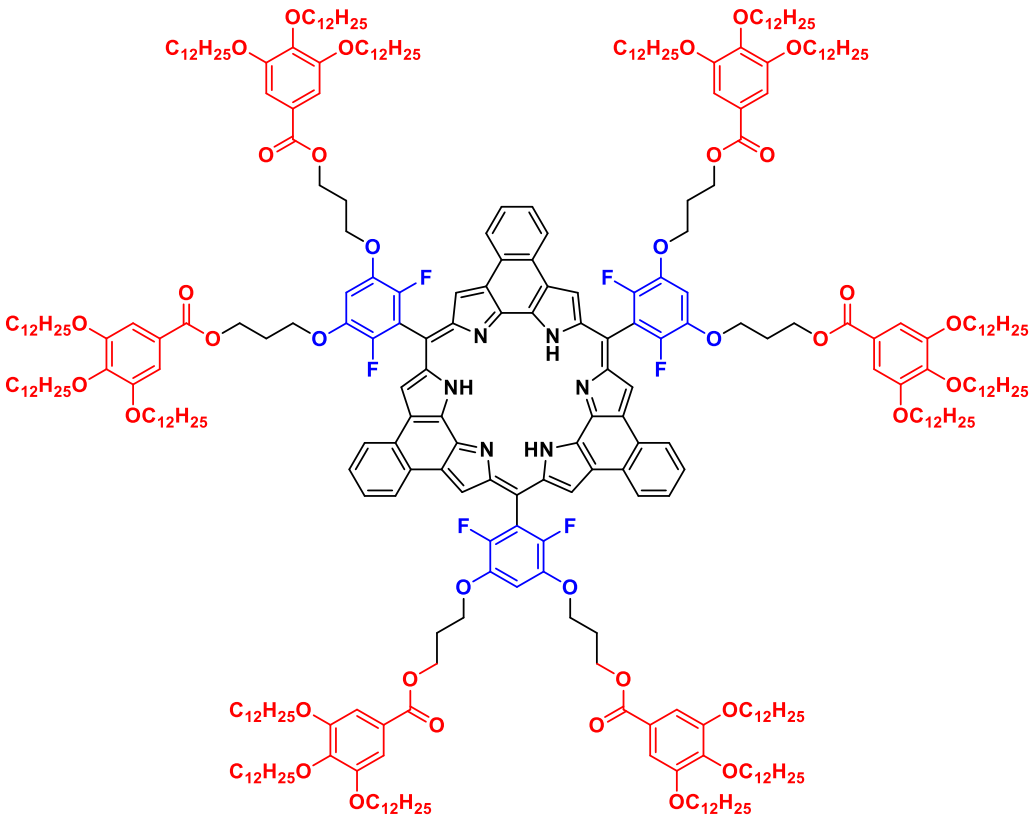

A 10 mL vial was charged with **NRos-6** (10 mg, 5.53 µmol, 1 equiv.), 3,4,5-tris(dodecyloxy)benzoic acid (44.84 mg, 86.41 µmol, 12 equiv.), and $KHCO_3$ (11.08 mg, 110.69 µmol, 20 equiv.) Then dry DMF (2 mL) was added to dissolve the solids. The reaction mixture was stirred at 60°C for 16 hours. Hexanes (30 mL) were added, and the reaction mixture was washed with brine (20 mL x 3), water (20 mL), and DMF. The collected organic fraction was dried over Na_2SO_4, and the volatiles were fully evaporated off. The crude product obtained in this way was purified via silica gel column chromatography using a gradient of hexanes: ethyl acetate = 8:1 to 6/1 as the eluent. The product was further purified via size exclusion chromatography (Bio-Beads™ S-X1) using dichloromethane as the eluent to obtain, after drying, the target compound as a dark purple oily solid. **Yield** 13.37 mg, 45%. **^{1}H NMR** (600 MHz, THF-d_8): δ (ppm) = 7.25 (s, 12H), 7.03 (dd, J = 6.1, 3.3 Hz, 6H), 6.89 (dd, J = 6.0, 3.5 Hz, 6H), 6.82 (t, J = 8.0 Hz, 3H), 5.09 (s, 6H), 4.40 (d, J = 6.6 Hz, 12H), 4.09 (t, J = 6.2 Hz, 12H), 3.99 (t, 36H), 2.17 (p, J = 6.2 Hz, 12H), 1.87 – 1.81 (m, 36H), 1.57 – 1.54 (m, 36H), 1.33 – 1.28 (m, 288H), 0.90 (d, J = 5.0 Hz, 54H). **^{13}C NMR** (151 MHz, THF-d_8): δ (ppm) = 166.54, 154.10, 145.23, 144.17, 143.96, 143.61, 133.19, 132.08, 130.36, 126.79, 125.90, 124.99, 124.46, 120.61, 114.49, 109.11, 105.44, 73.95, 70.09, 62.50, 33.10, 33.08, 31.60, 30.98, 30.94, 30.90, 30.87, 30.81, 30.79, 30.77, 30.75, 30.69, 30.66, 30.59, 30.56, 30.51, 30.48, 30.08, 27.37, 27.33, 23.78, 23.76, 14.67, 14.64. **^{19}F NMR** (564 MHz, THF-d_8): δ (ppm) = -139.35. **UV-Vis** (DCM): λ_{max} (nm) (log ε($dm^3\ cm^{-1}\ mol^{-1}$)): 476 (5.0), 583 (4.8). MS (MALDI-TOF, DCTB): m/z [M+H$^+$] Calculated for $C_{339}H_{522}F_6N_6O_{36}$: 5368.9, found: 5369.0.

3. NMR spectra

4-(3-Bromopropoxy)-2,6-difluorobenaldehyde

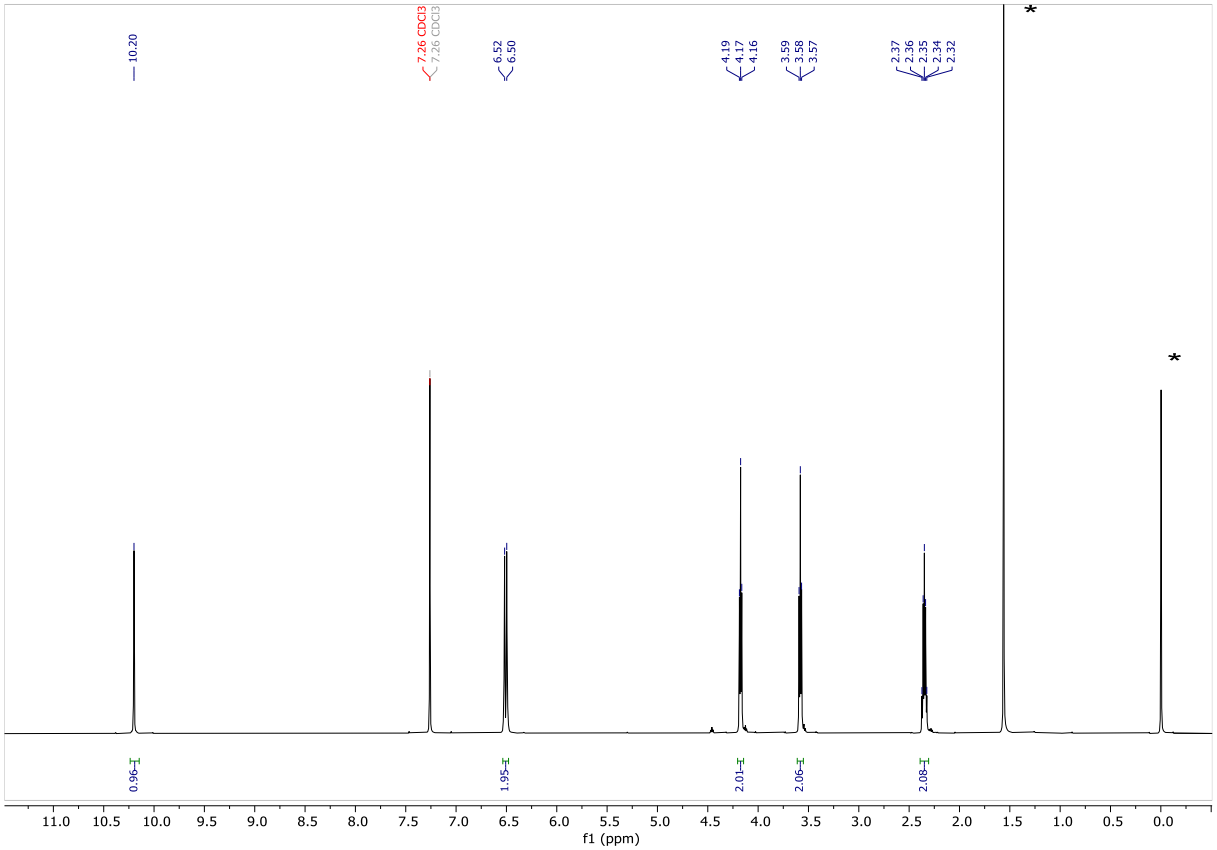

Figure S3.1. ^{1}H NMR spectrum ($CDCl_3$) of **4-(3-bromopropoxy)-2,6-difluorobenaldehyde**

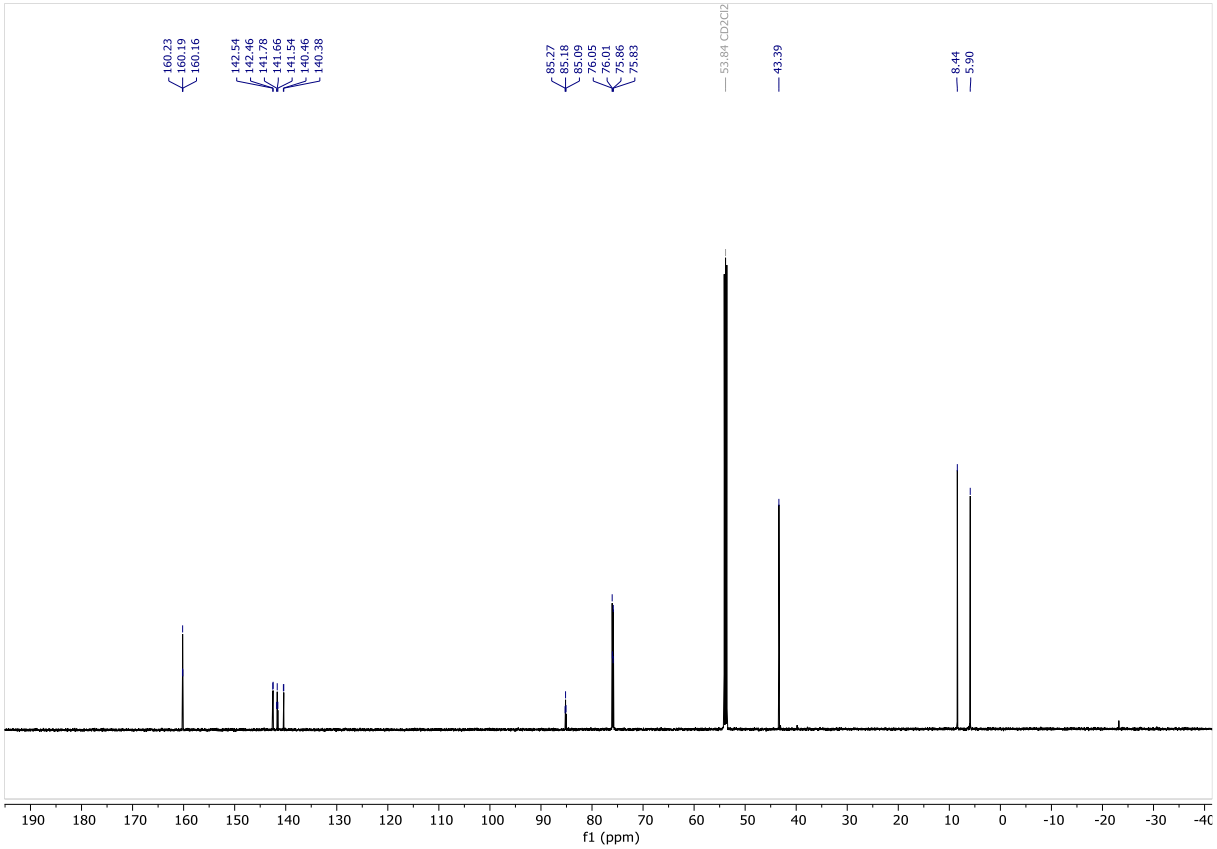

Figure S3.2. ^{13}C NMR spectrum ($CDCl_3$) of **4-(3-bromopropoxy)-2,6-difluorobenaldehyde**

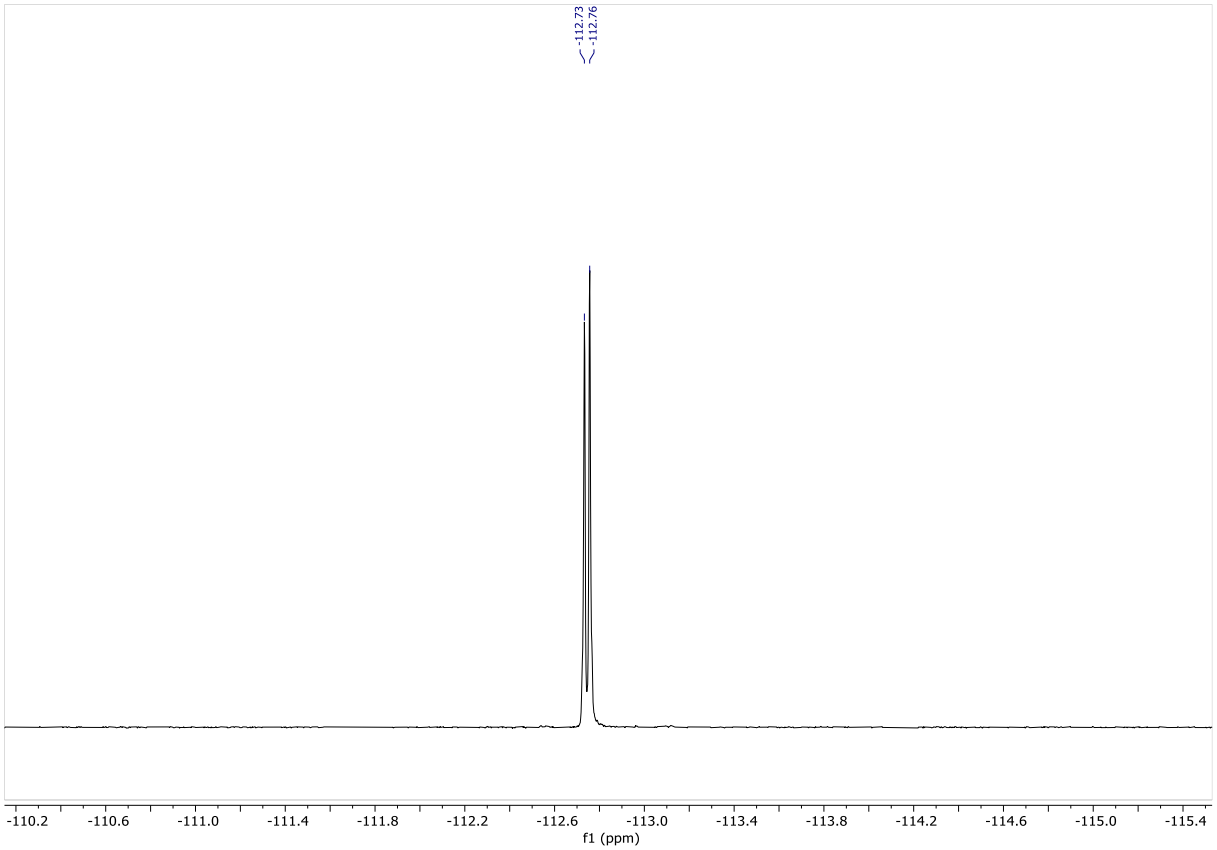

Figure S3.3. ^{19}F NMR spectrum ($CDCl_3$) of **4-(3-bromopropoxy)-2,6-difluorobenaldehyde**

4-(3-Bromopropoxy)-3,5-difluorobenaldehyde

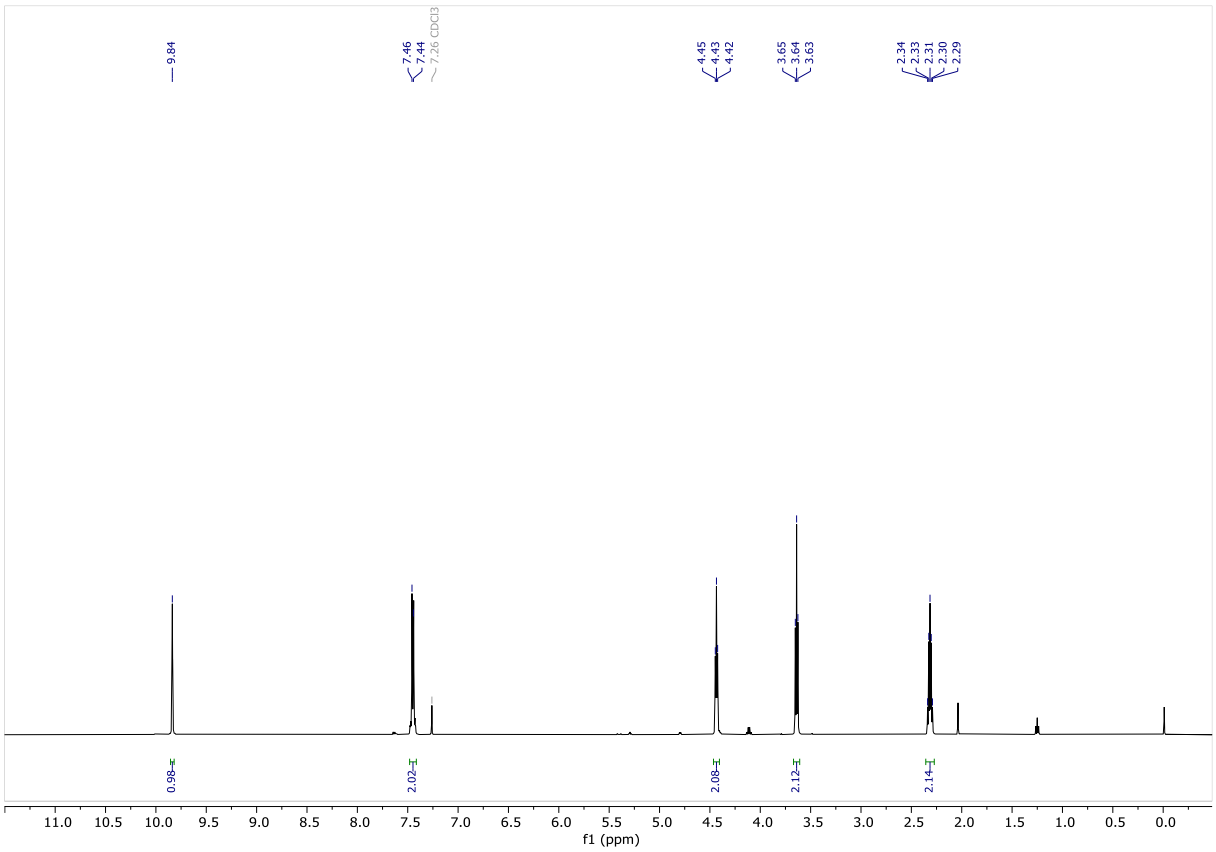

Figure S3.4. ^{1}H NMR spectrum ($CDCl_3$) of **4-(3-bromopropoxy)-2,6-difluorobenaldehyde**

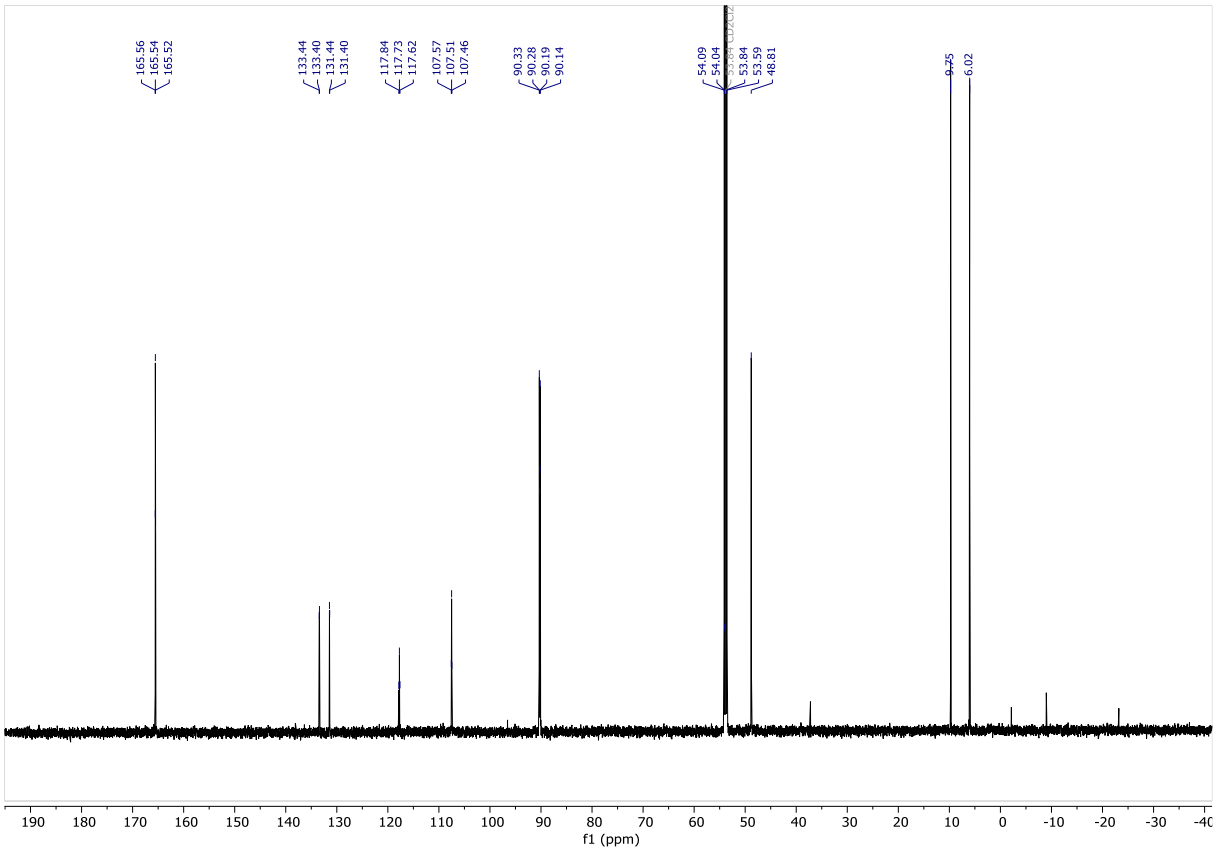

Figure S3.5. ^{13}C NMR spectrum ($CDCl_3$) of **4-(3-bromopropoxy)-2,6-difluorobenaldehyde**

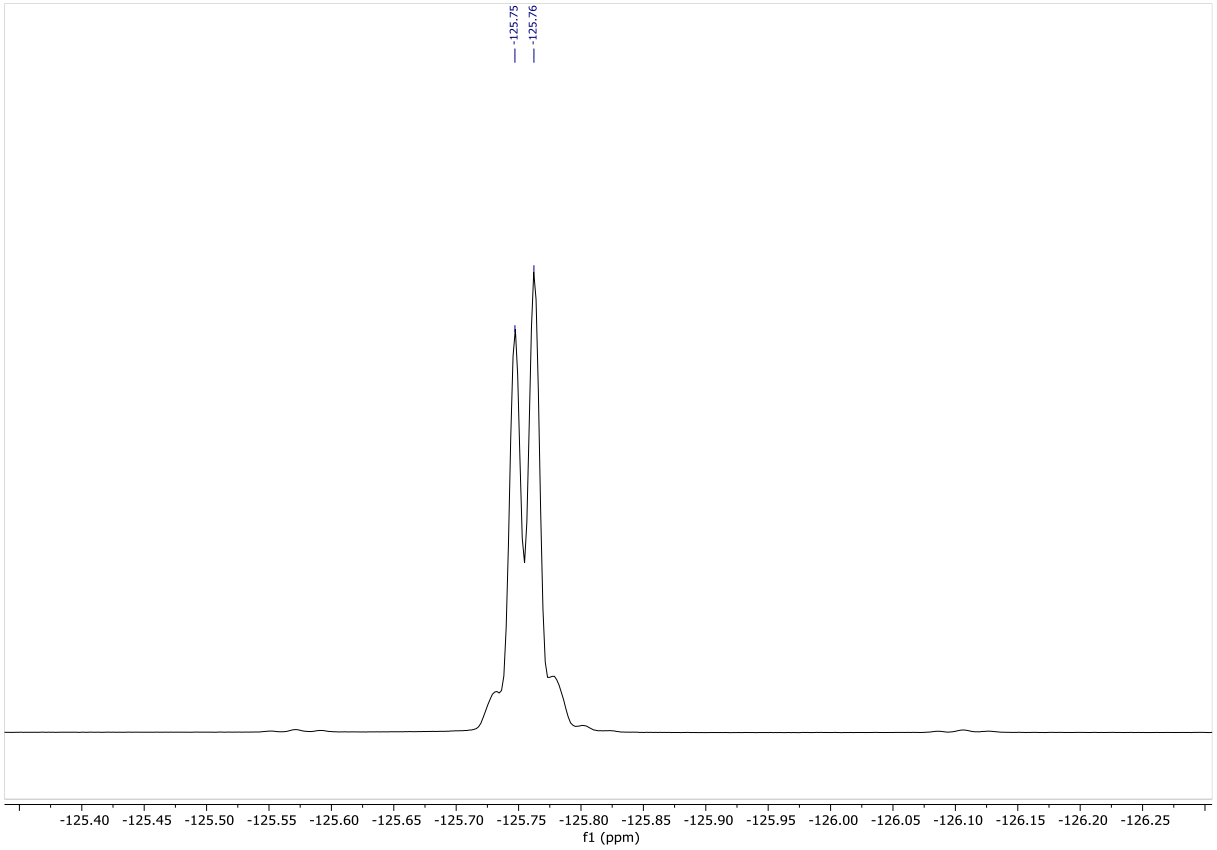

Figure S3.6. ^{19}F NMR spectrum ($CDCl_3$) of **4-(3-bromopropoxy)-2,6-difluorobenaldehyde**

3,5-bis(3-bromopropoxy)-2,6-difluorobenaldehyde

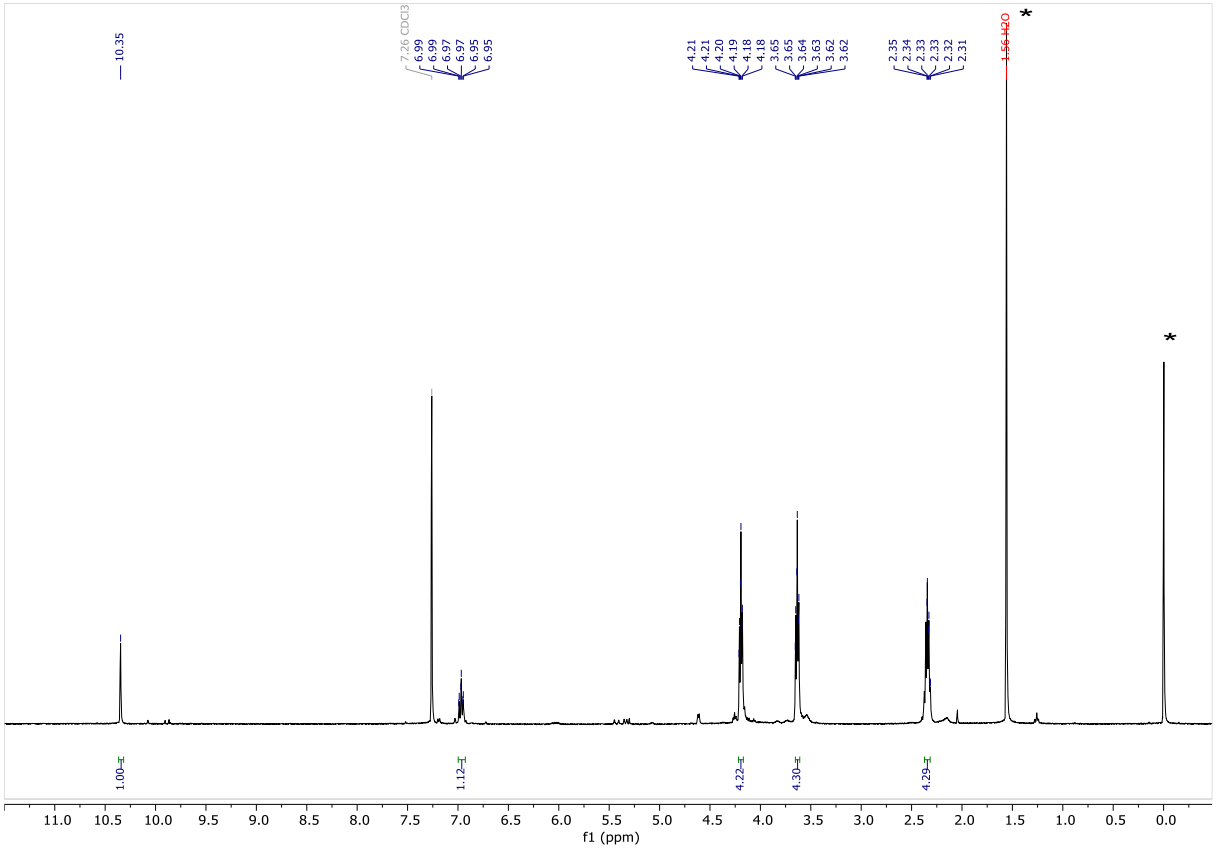

Figure S3.7. ^{1}H NMR spectrum ($CDCl_3$) of **3,5-bis(3-bromopropoxy)-2,6-difluorobenaldehyde**

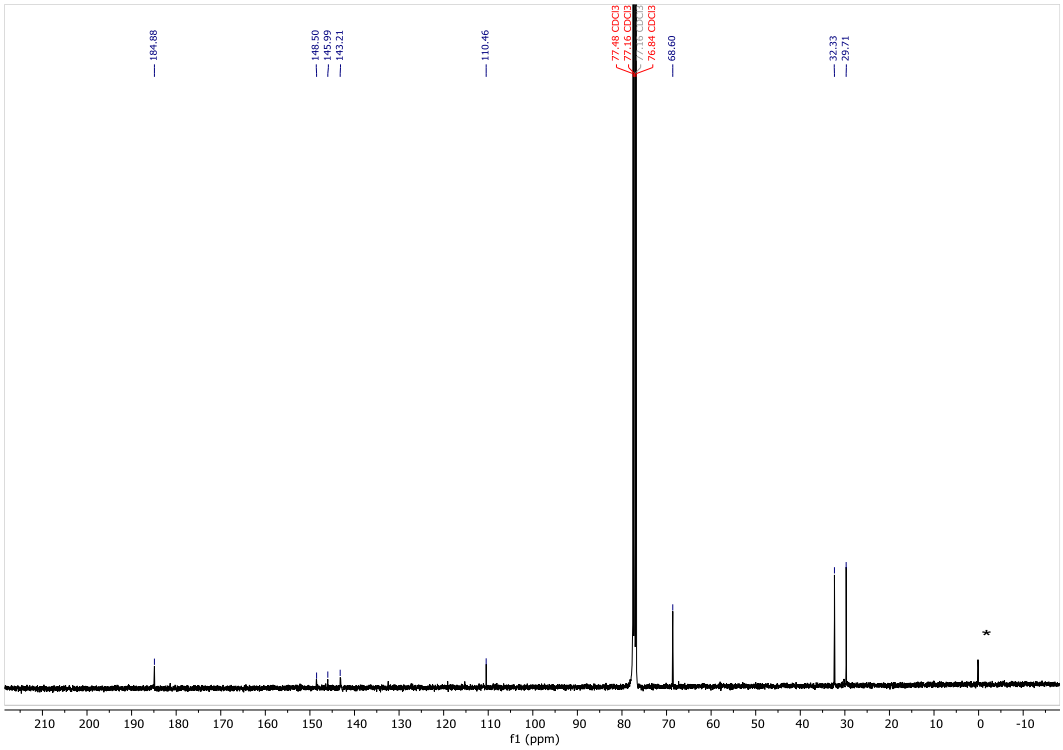

Figure S3.8. ^{13}C NMR spectrum ($CDCl_3$) of **3,5-bis(3-bromopropoxy)-2,6-difluorobenaldehyde**

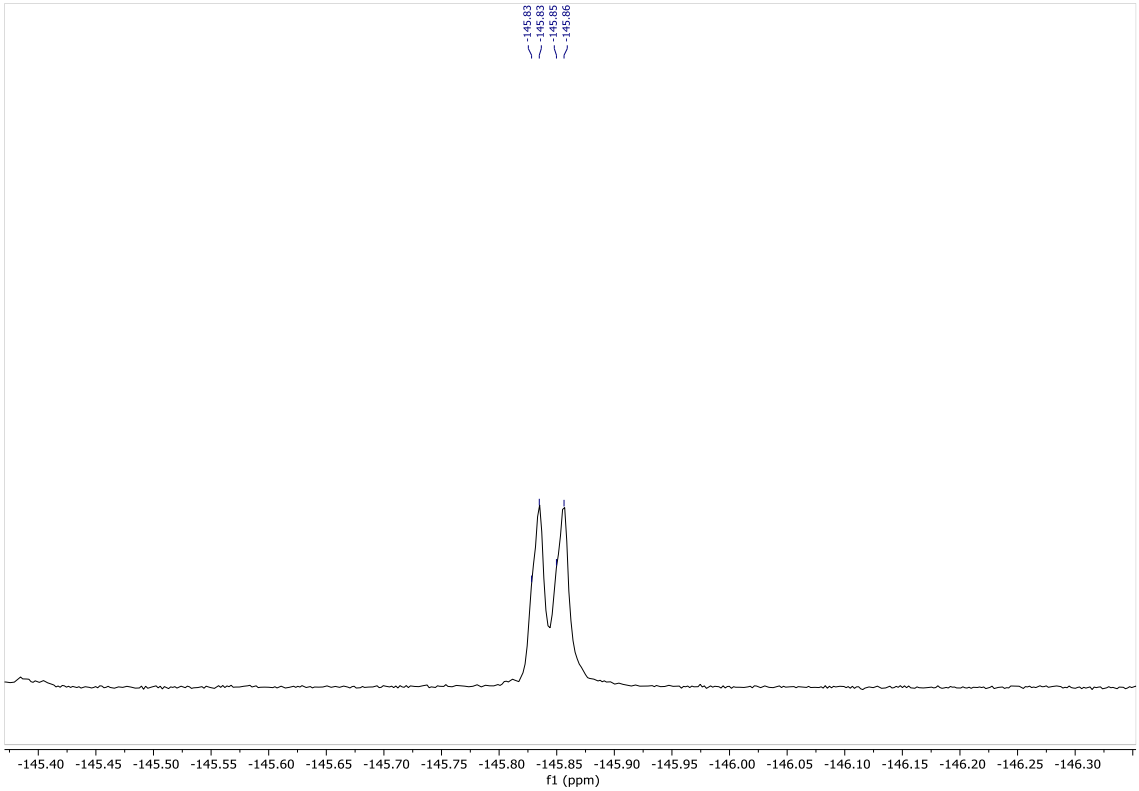

Figure S3.9. ^{19}F NMR spectrum ($CDCl_3$) of **3,5-bis(3-bromopropoxy)-2,6-difluorobenaldehyde**

NRos-4

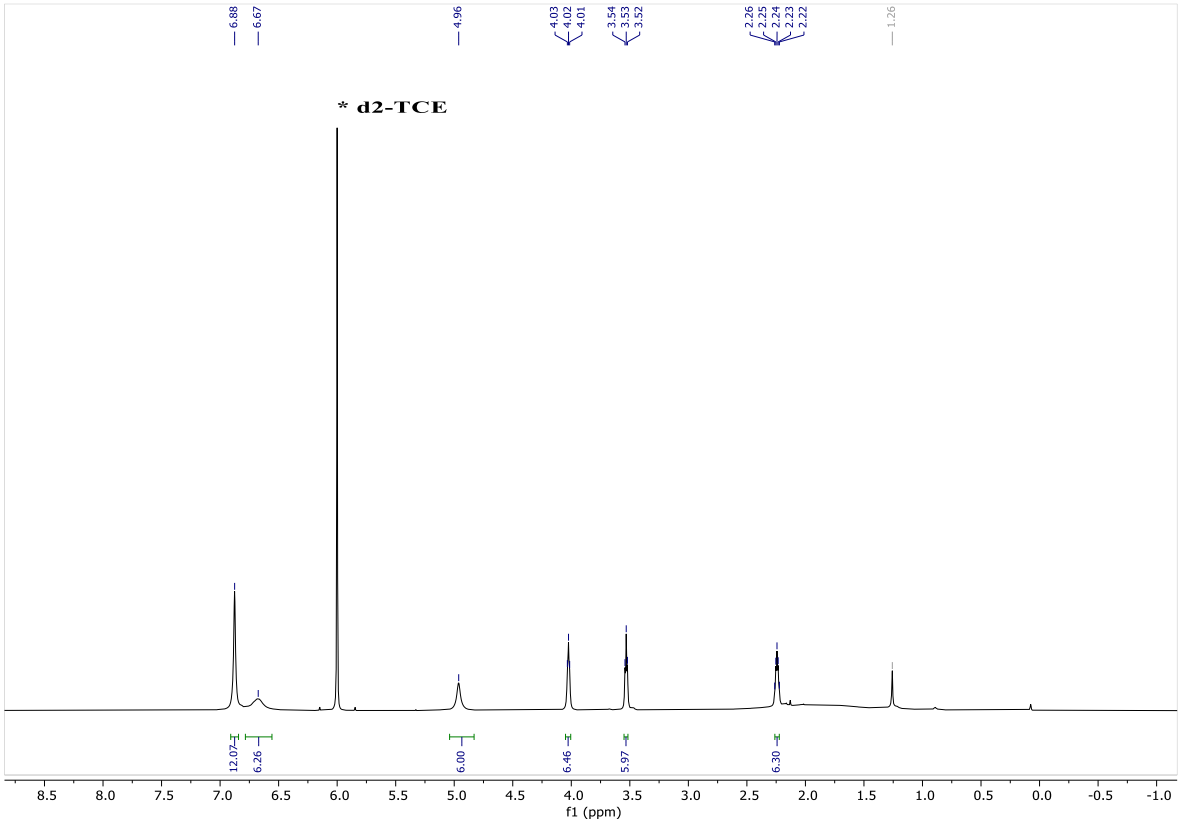

Figure S3.10. ^{1}H NMR spectrum (TCE-d_2) of **NRos-4**

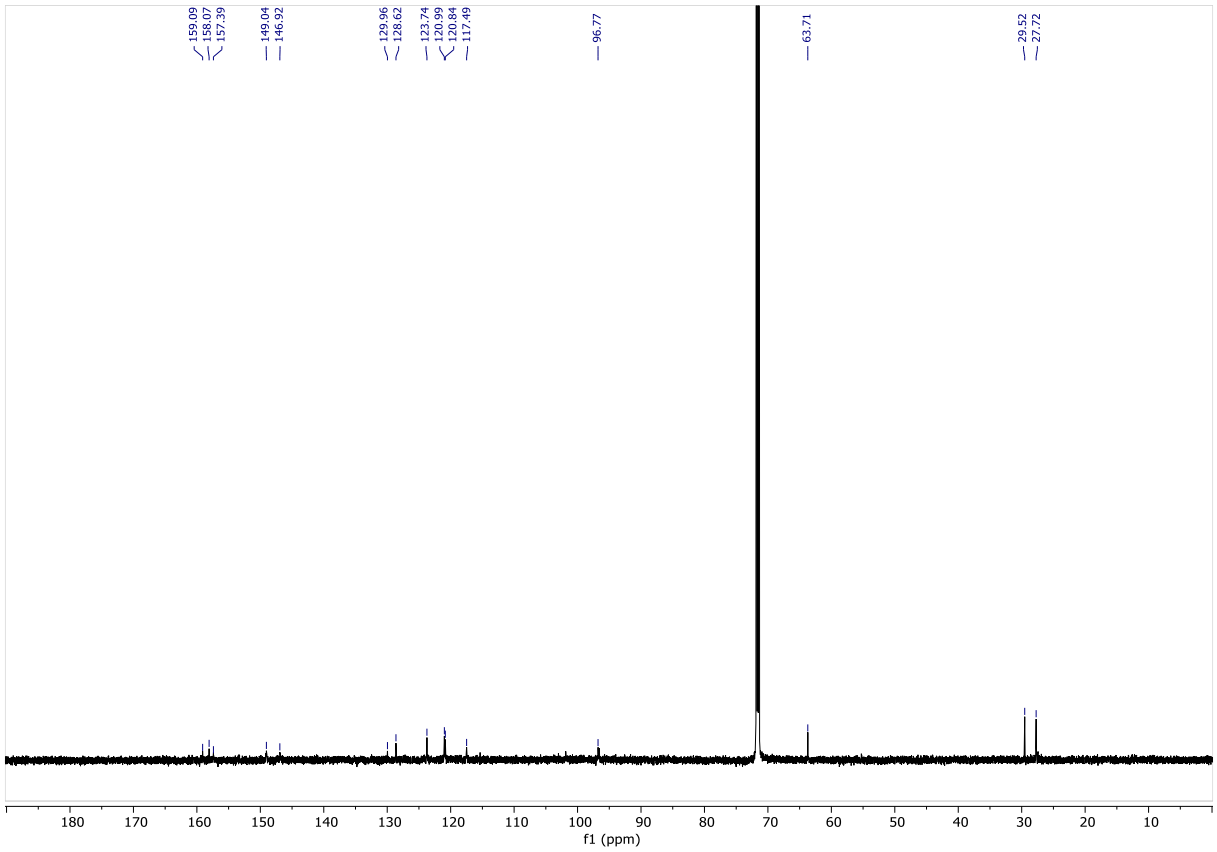

Figure S3.11. ^{13}C NMR (TCE-d_2) **NRos-4**

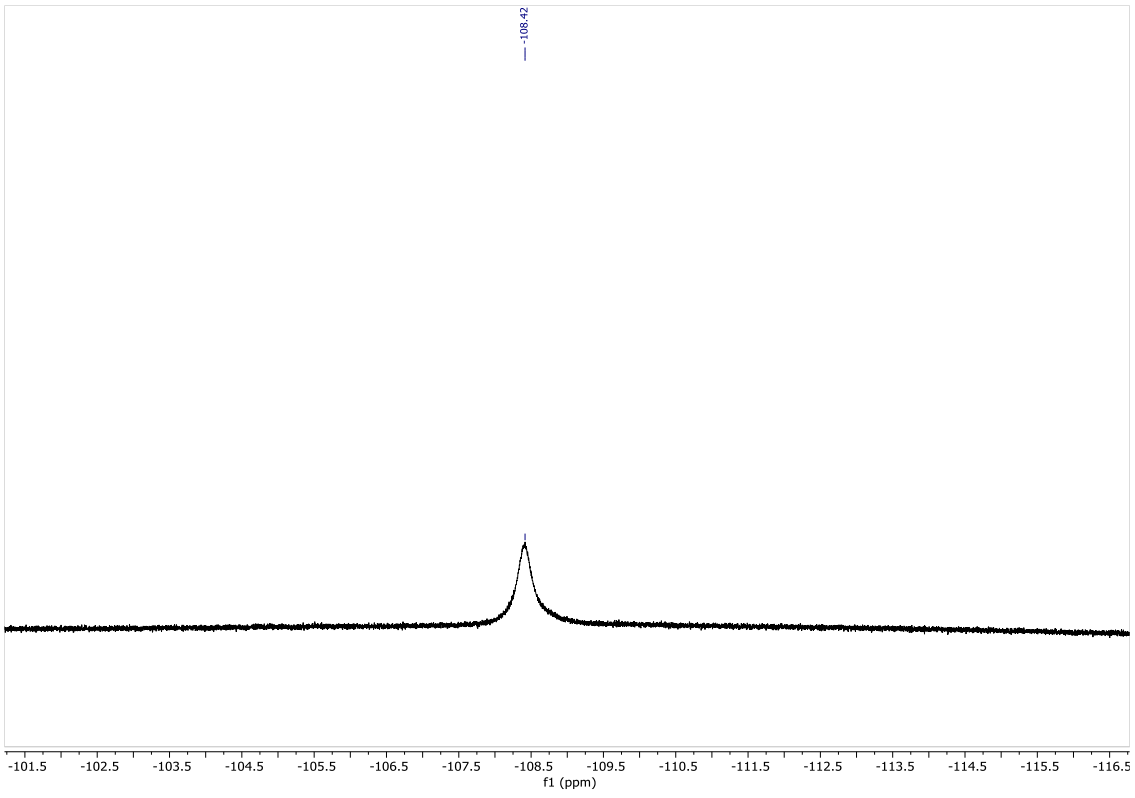

Figure S3.12. ^{19}F NMR (TCE-d_2) **NRos-4**

NRos-5

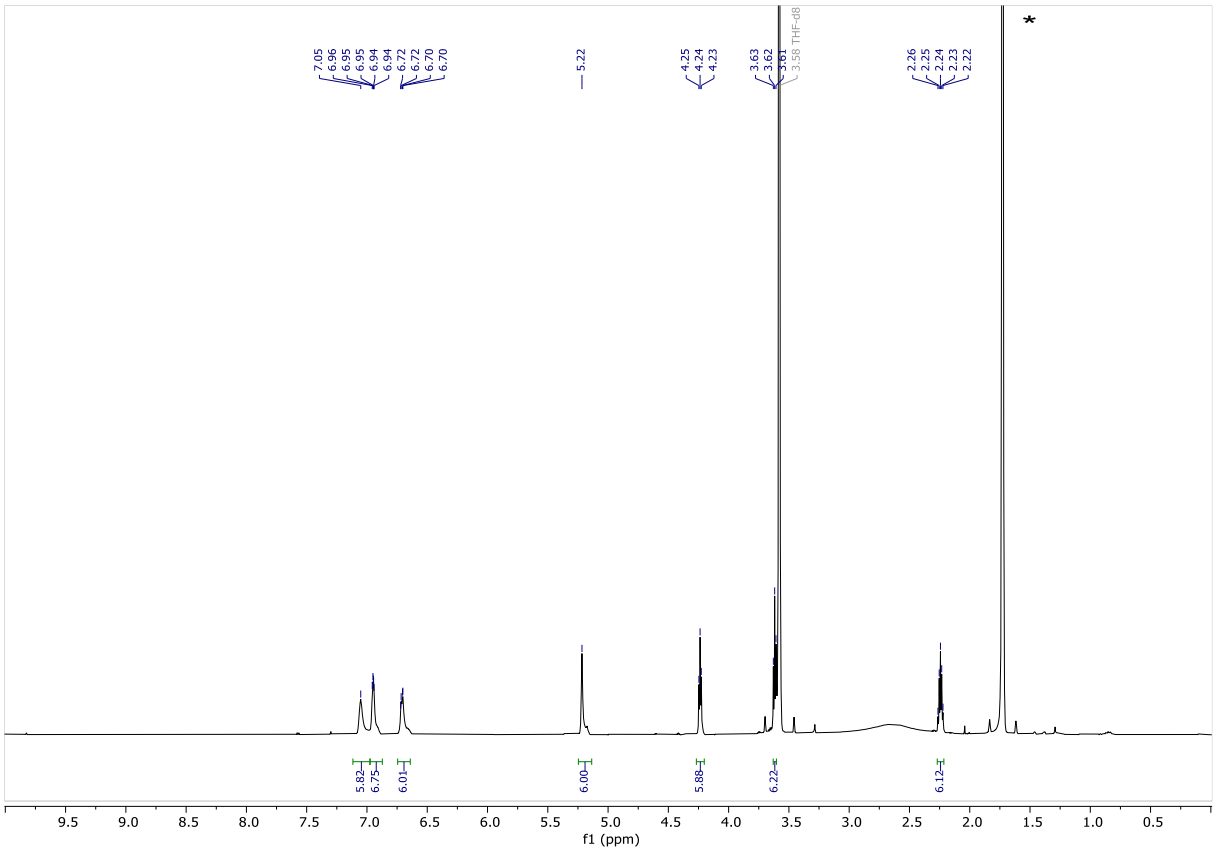

Figure S3.13. ^{1}H NMR spectrum (THF-d_8) of **NRos-5**

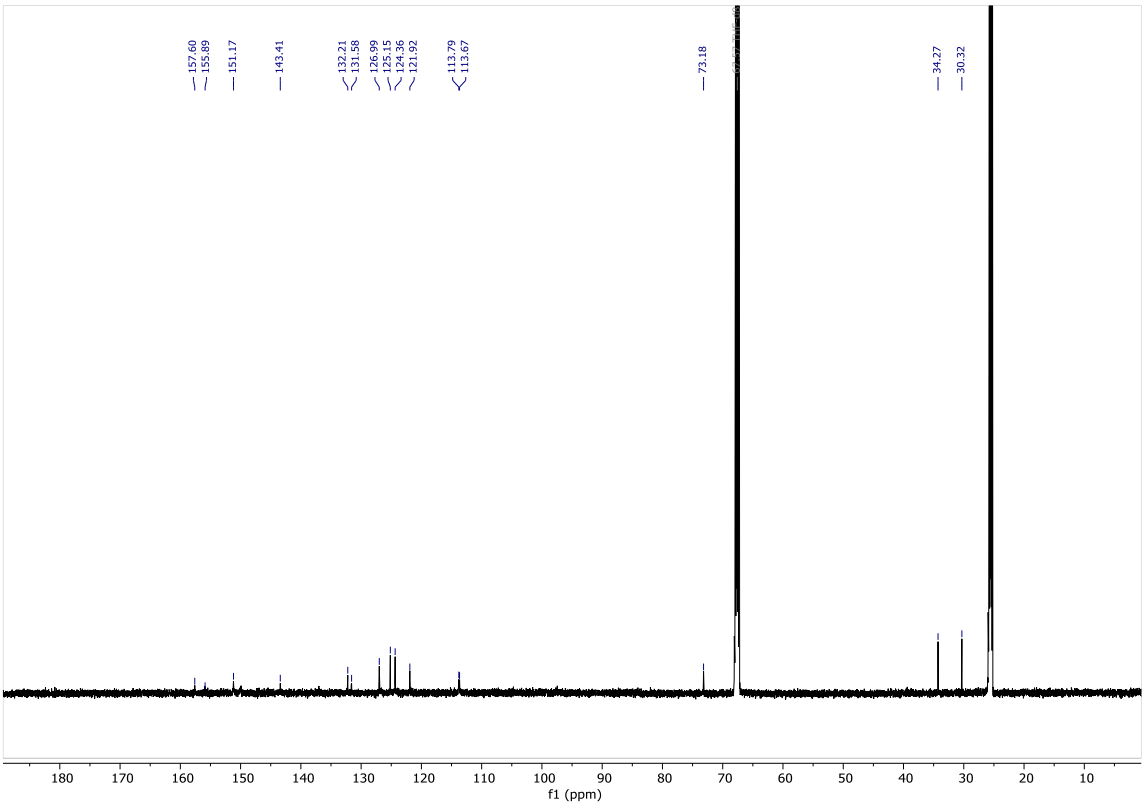

Figure S3.14. ^{13}C NMR spectrum (THF-d_8) of **NRos-5**

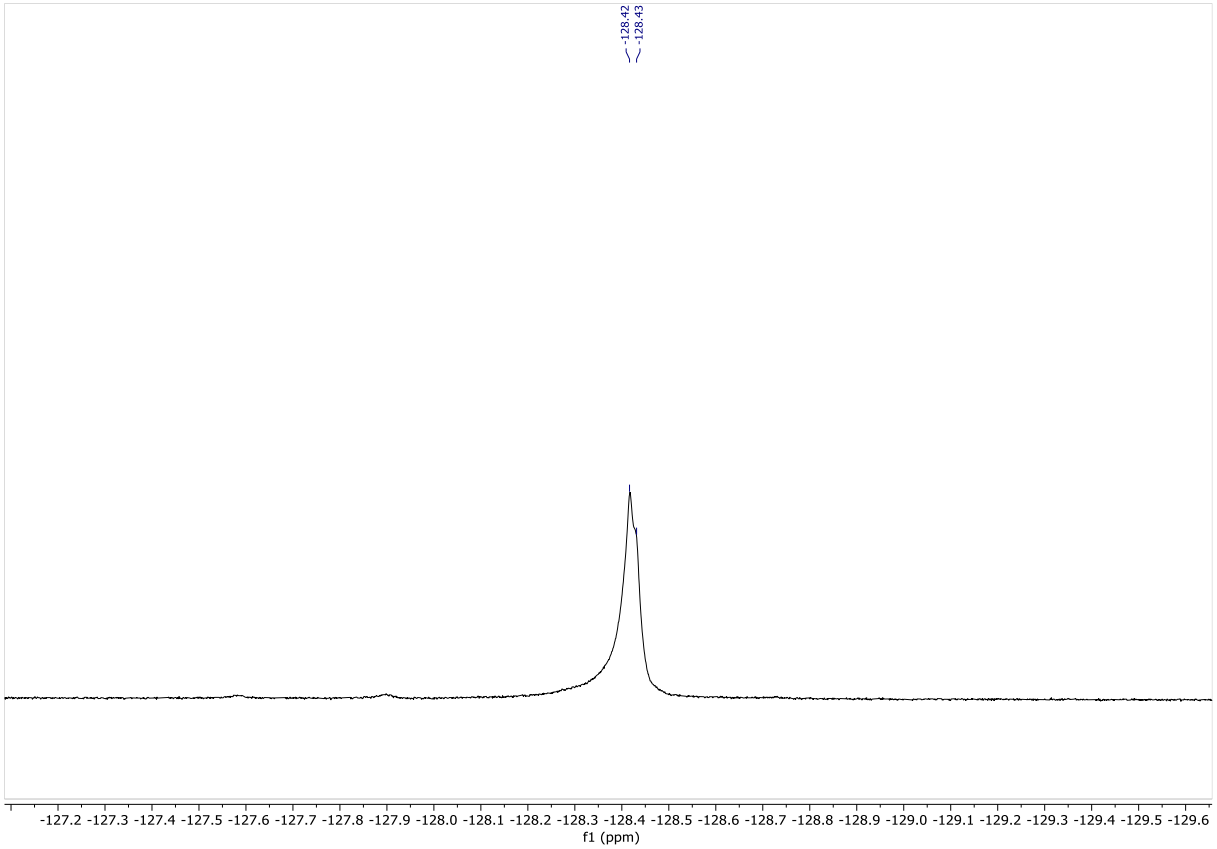

Figure S3.15. ^{19}F NMR spectrum (THF-d_8) of **NRos-5**

NRos-6

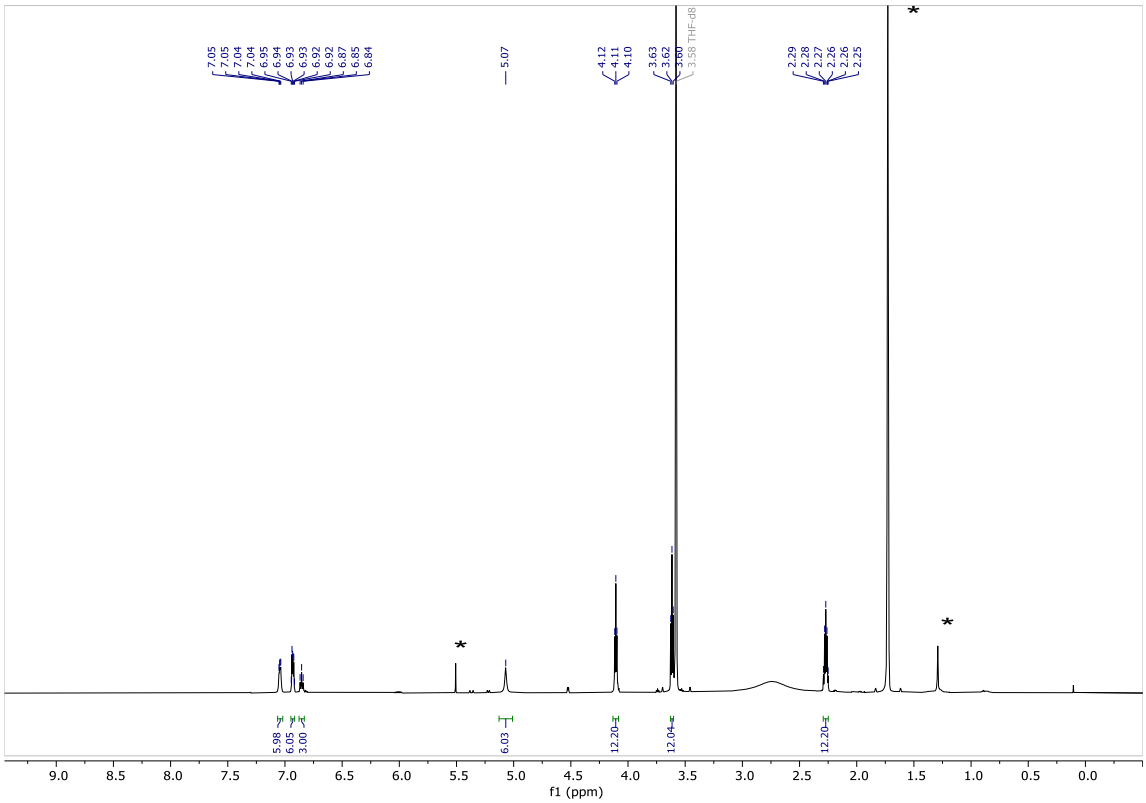

Figure S3.16. ^{1}H NMR spectrum (THF-d_8) of **NRos-6**

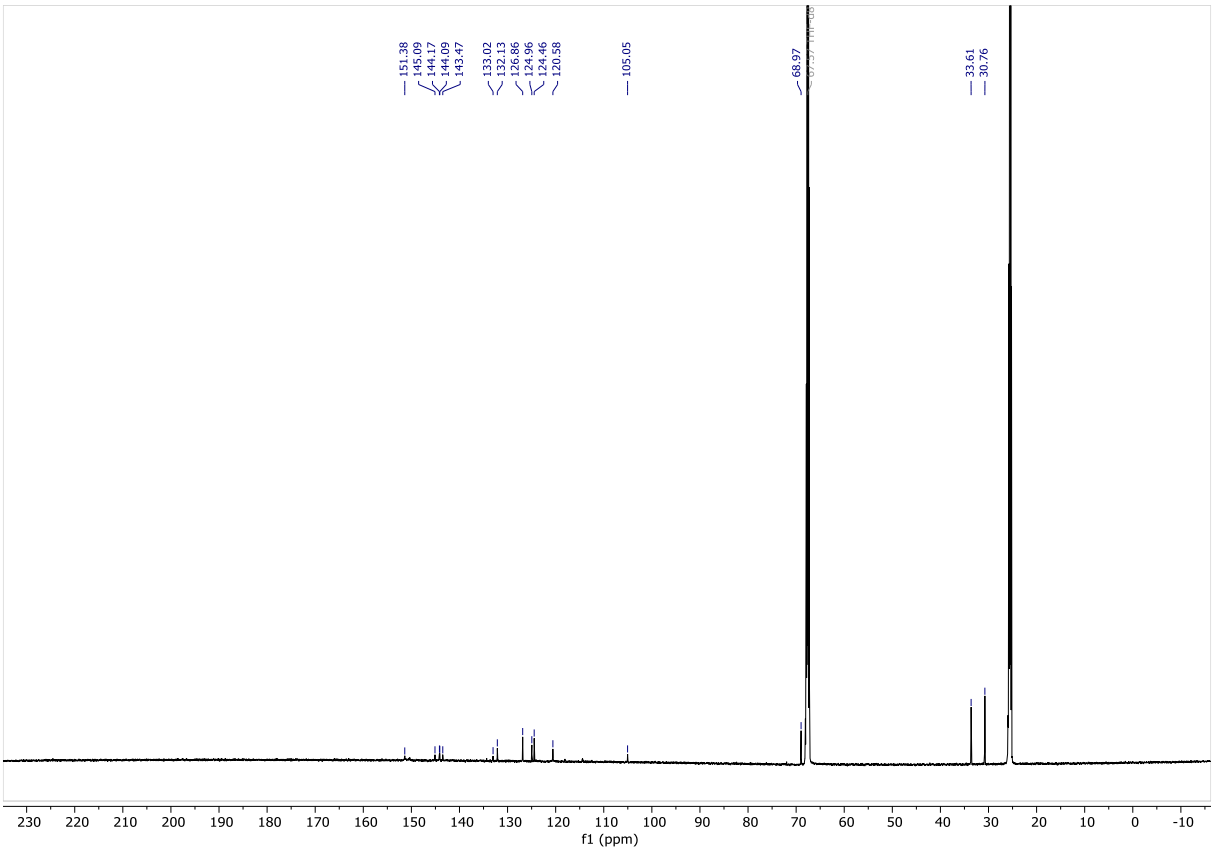

Figure S3.17. ^{13}C NMR spectrum (THF-d_8) of **NRos-6**

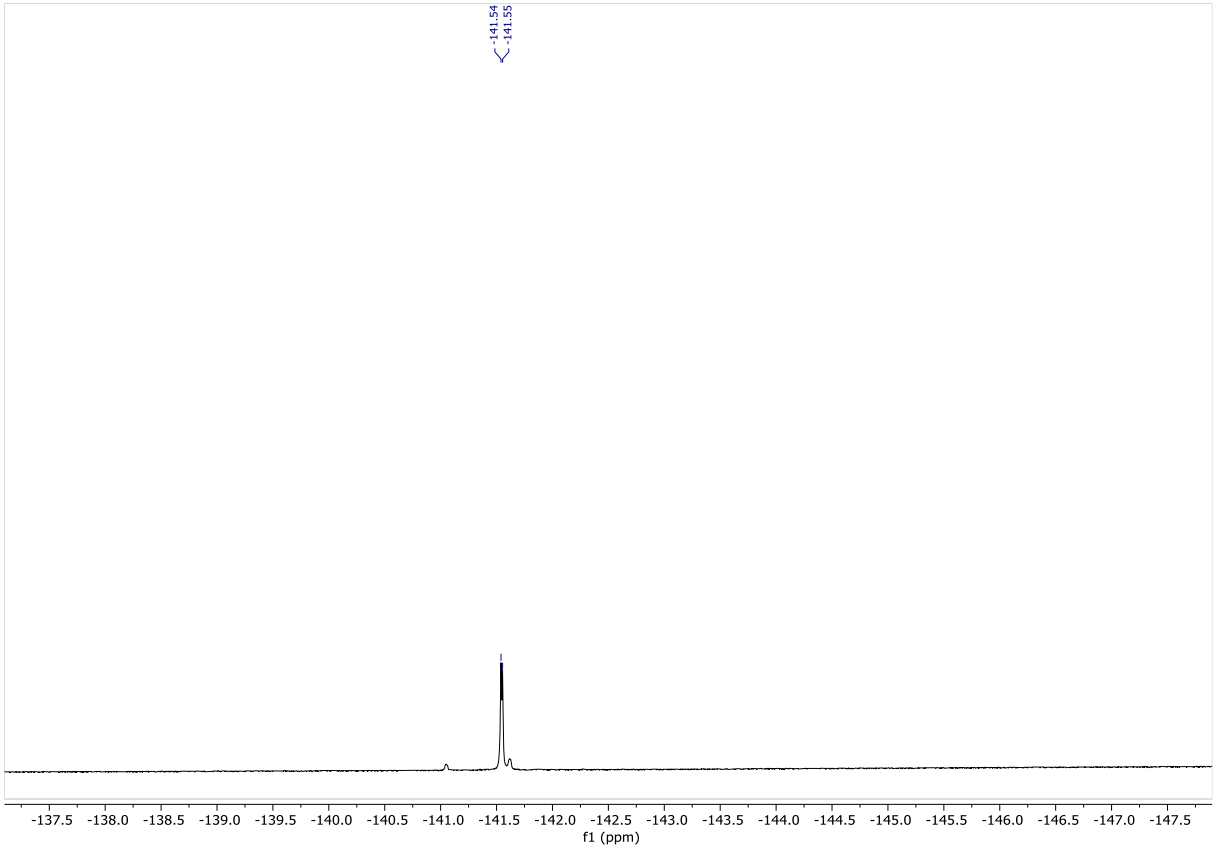

Figure S3.18. ^{19}F NMR spectrum (THF-d_8) of **NRos-6**

NRos-1

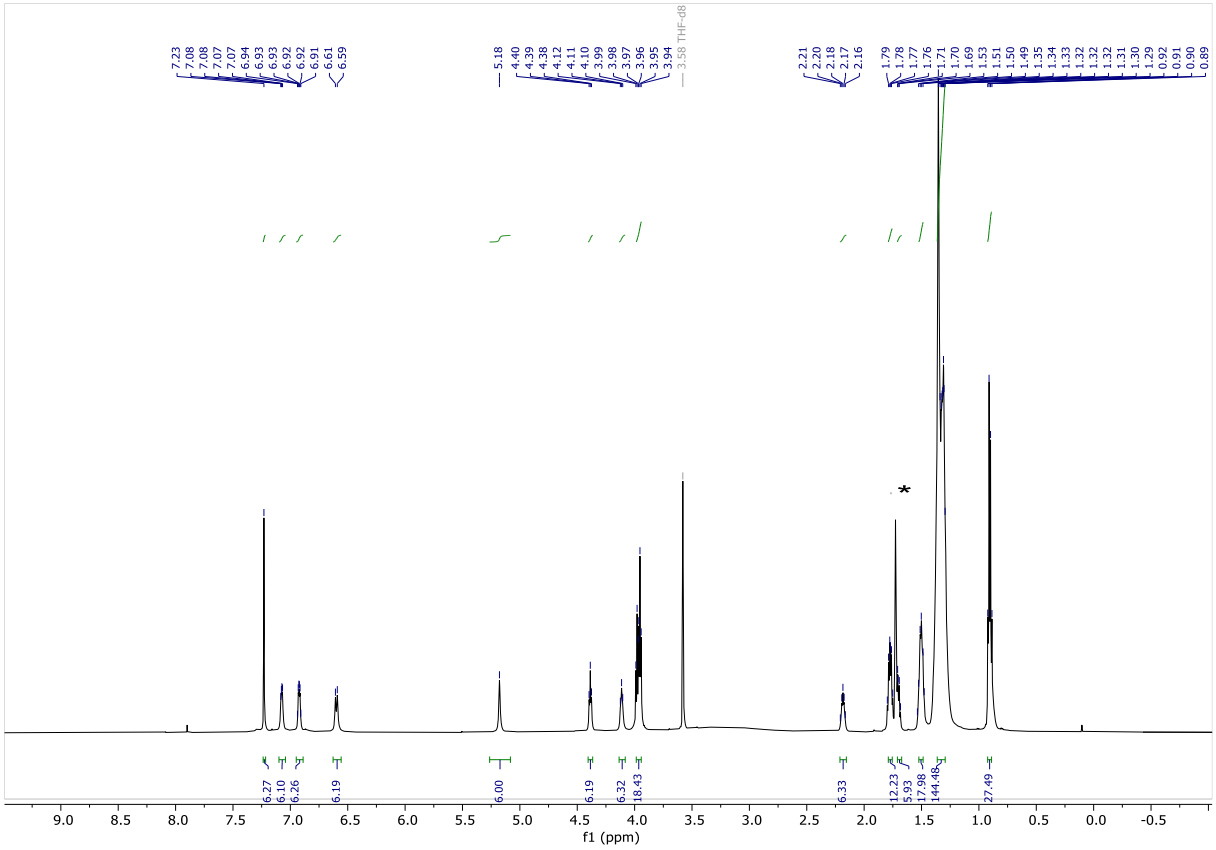

Figure S3.19. ^{1}H NMR spectrum (THF-d_8) of **NRos-1**

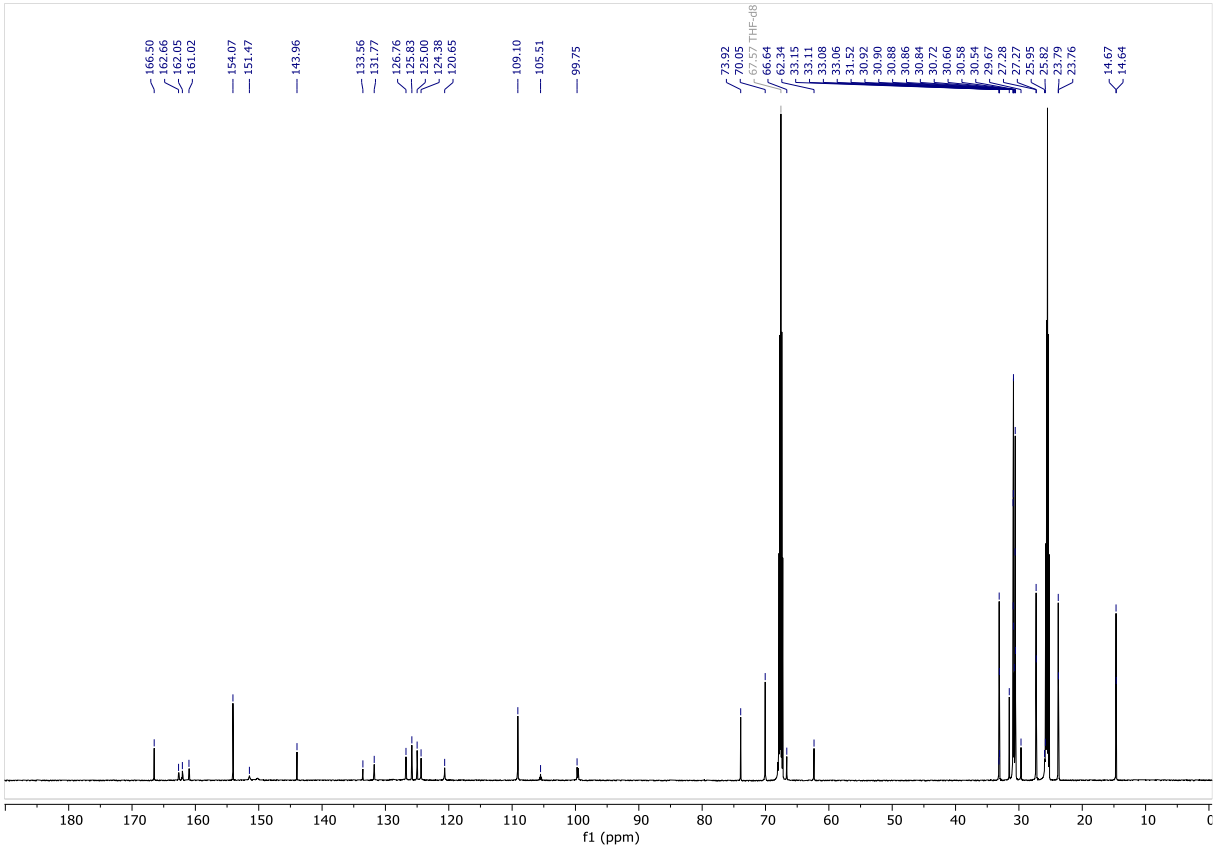

Figure S3.20. ^{13}C NMR spectrum (THF-d_8) of **NRos-1**

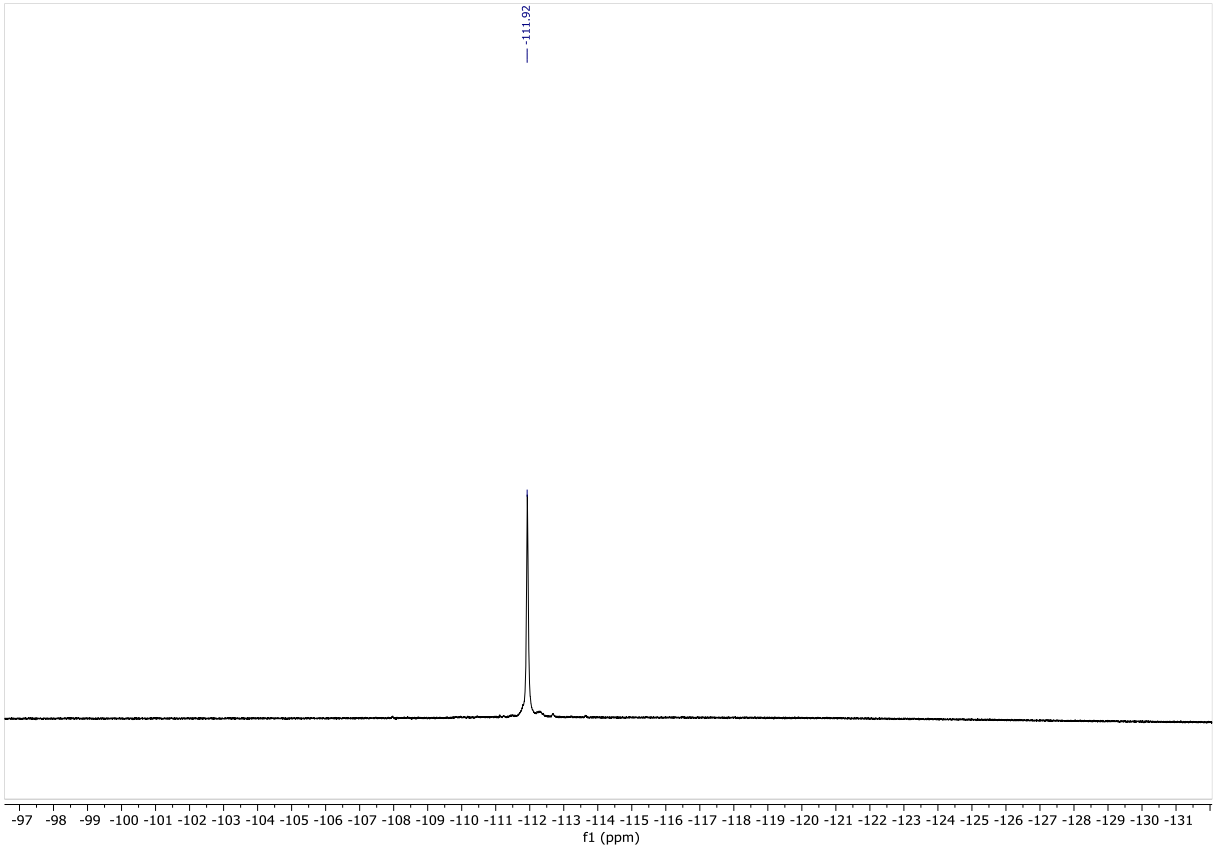

Figure S3.21. ^{19}F NMR spectrum (THF-d_8) of **NRos-1**

NRos-2

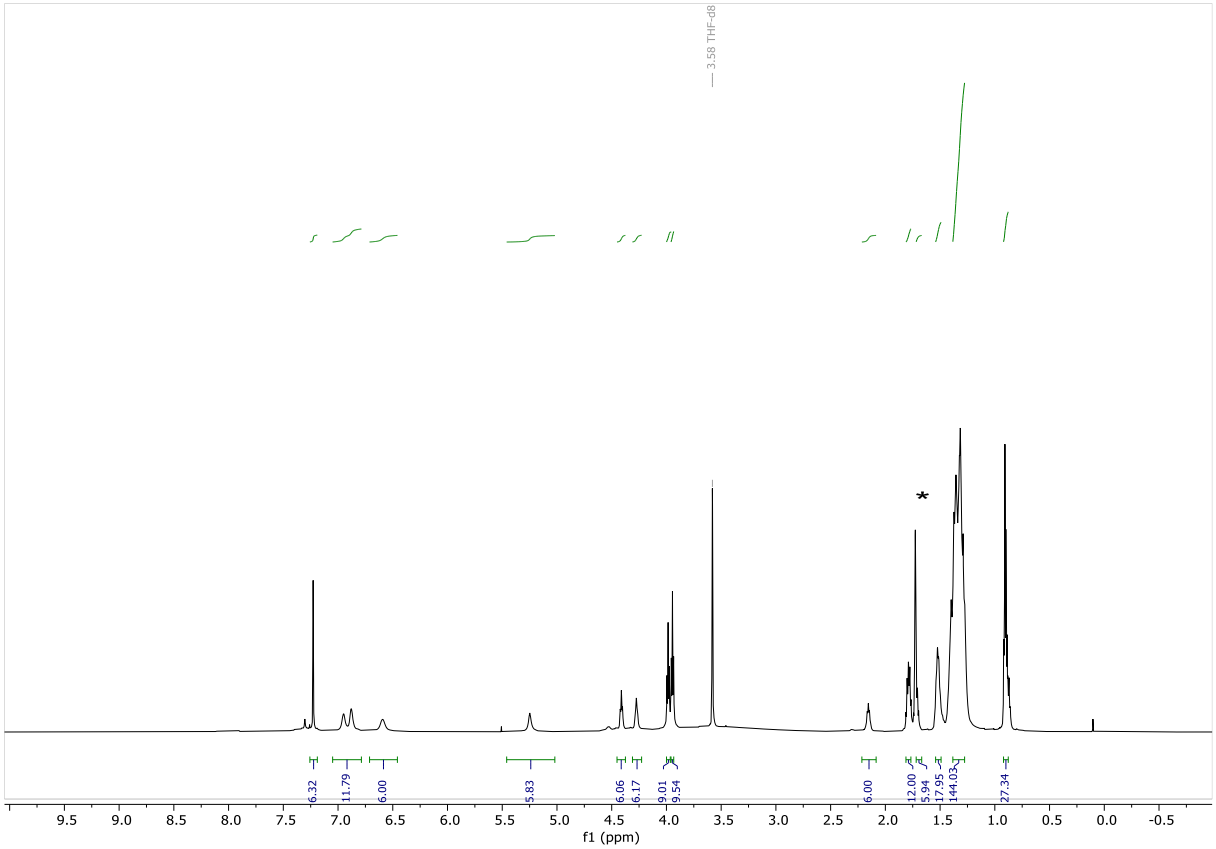

Figure S3.22. ^{1}H NMR spectrum (THF-d_8) of **NRos-2**

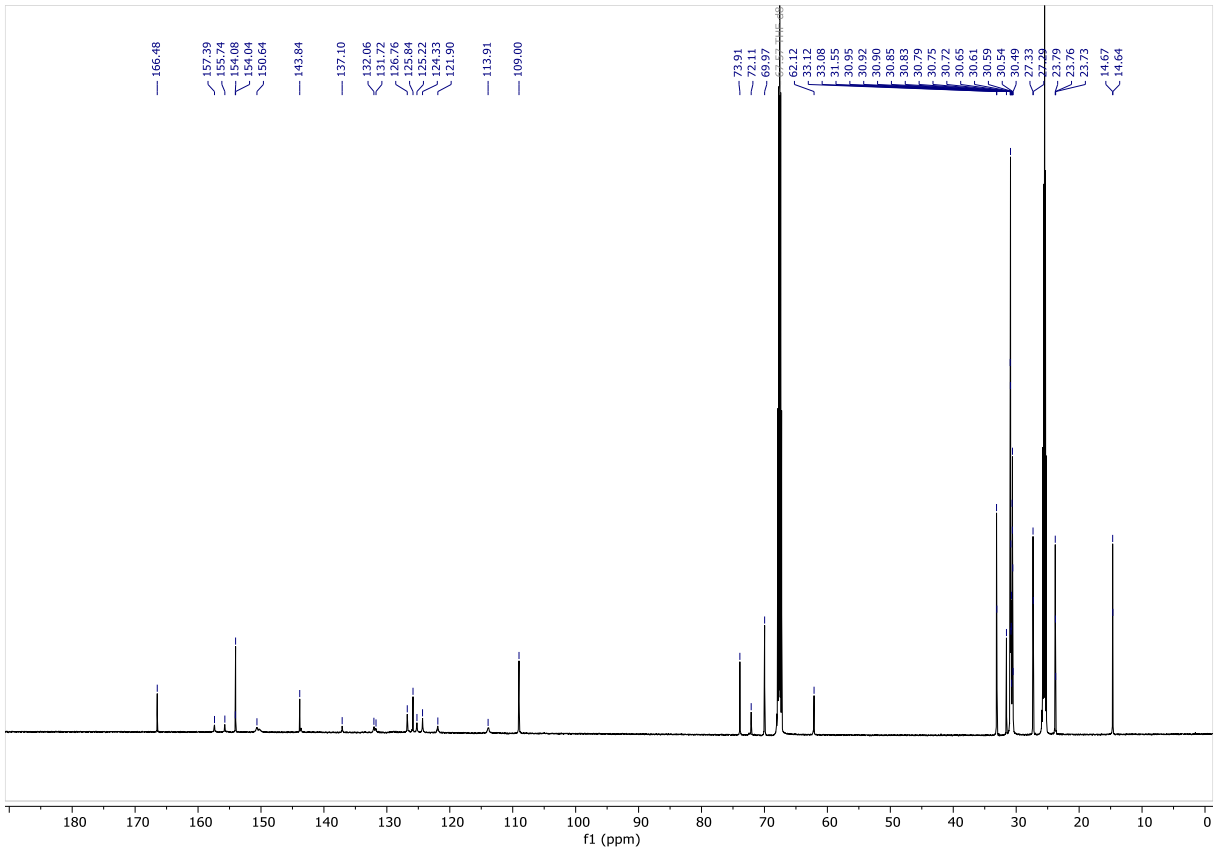

Figure S3.23. ^{13}C NMR spectrum (THF-d_8) of **NRos-2**

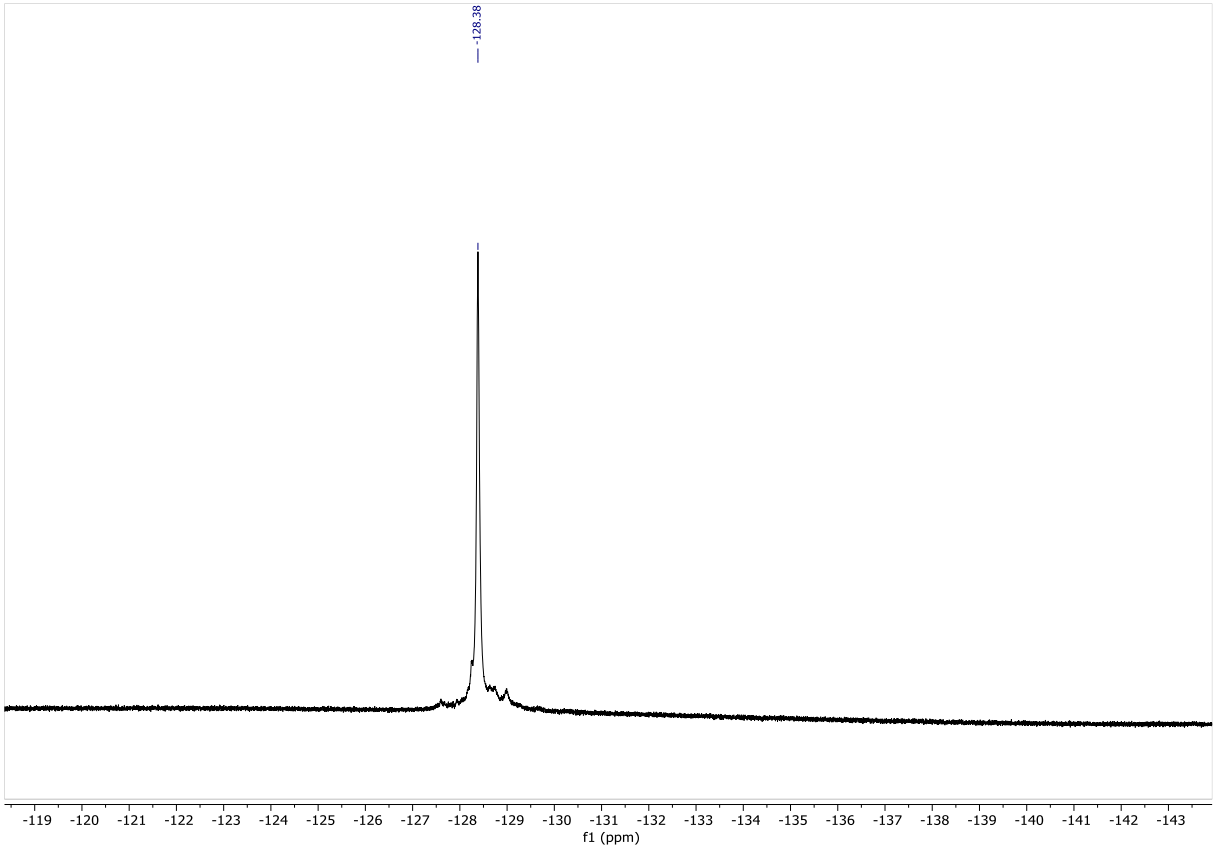

Figure S3.24. ^{19}F NMR spectrum (THF-d_8) of **NRos-2**

NRos-3

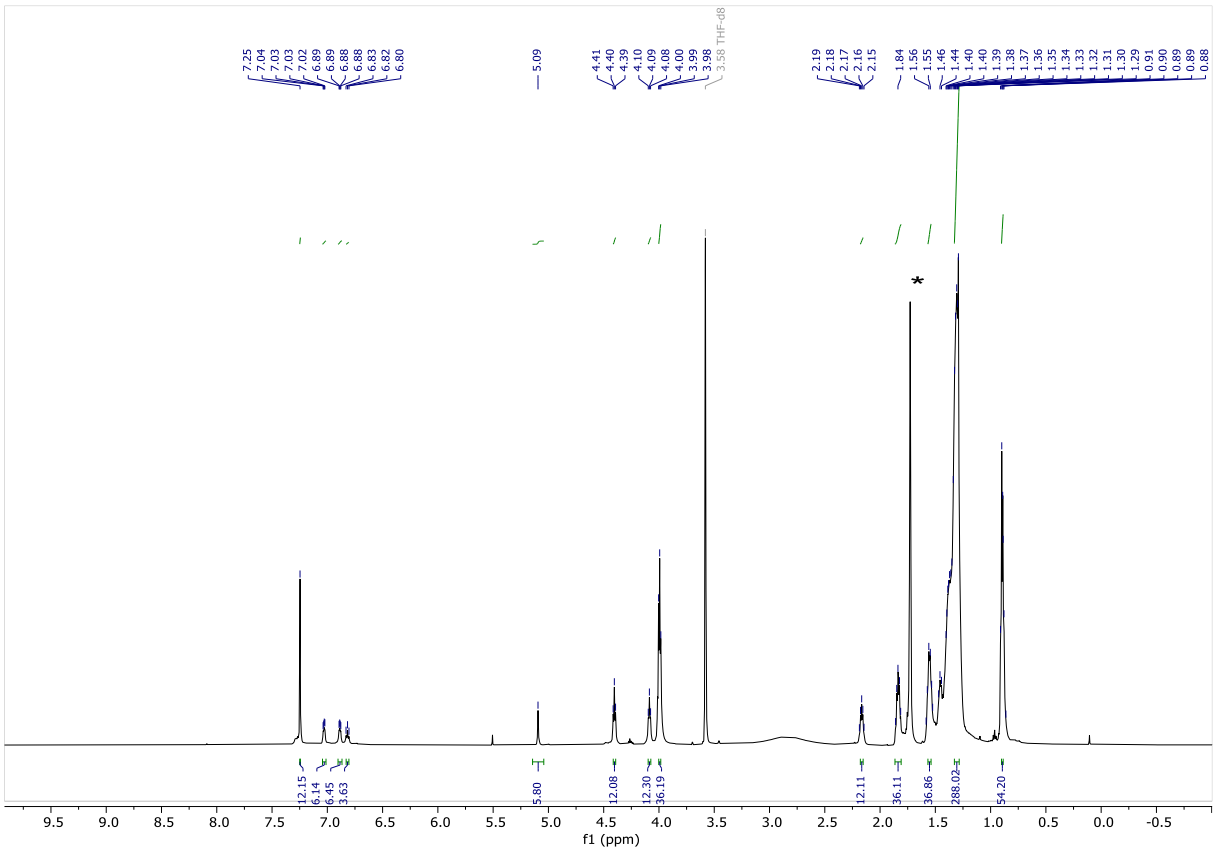

Figure S3.25. ^{1}H NMR spectrum (THF-d_8) of **NRos-3**

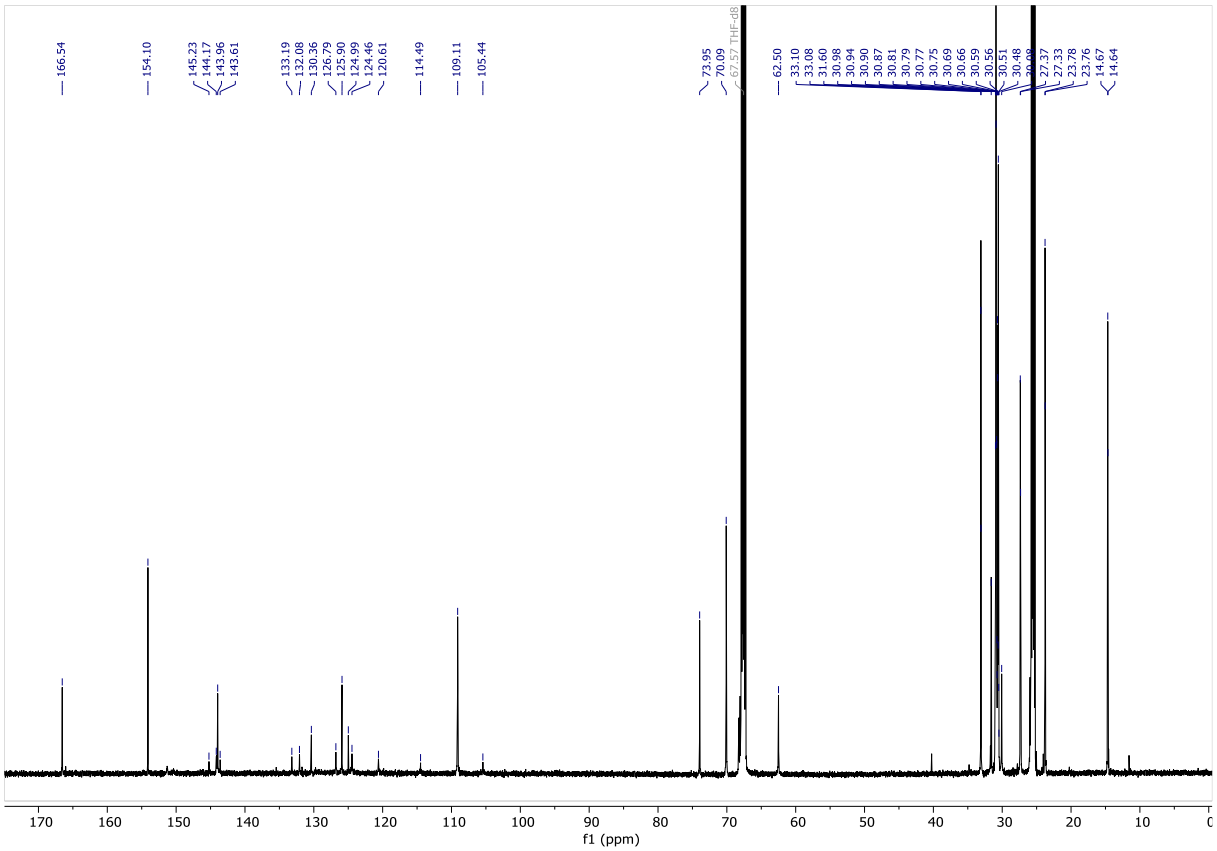

Figure S3.26. ^{13}C NMR spectrum (THF-d_8) of **NRos-3**

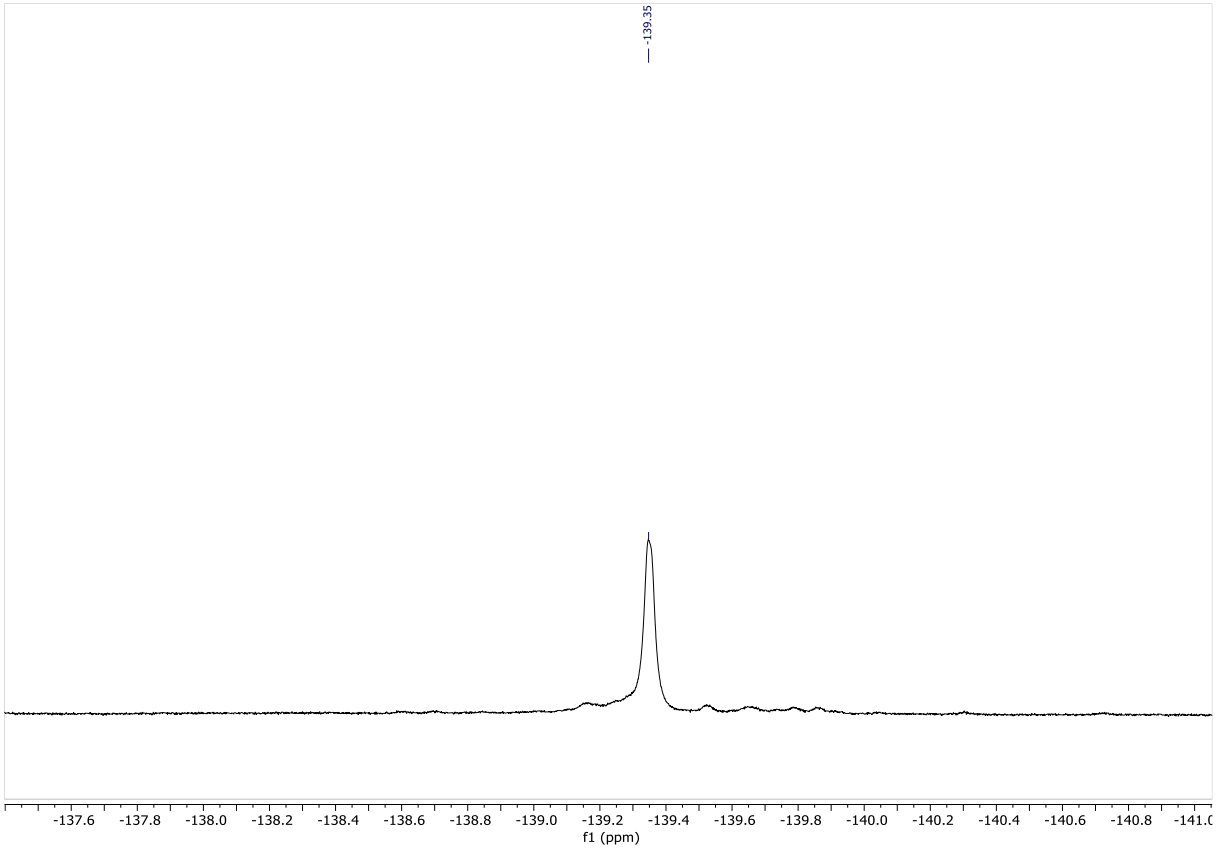

Figure S3.27. ^{19}F NMR spectrum (THF-d_8) of **NRos-3**

4. Mass spectra

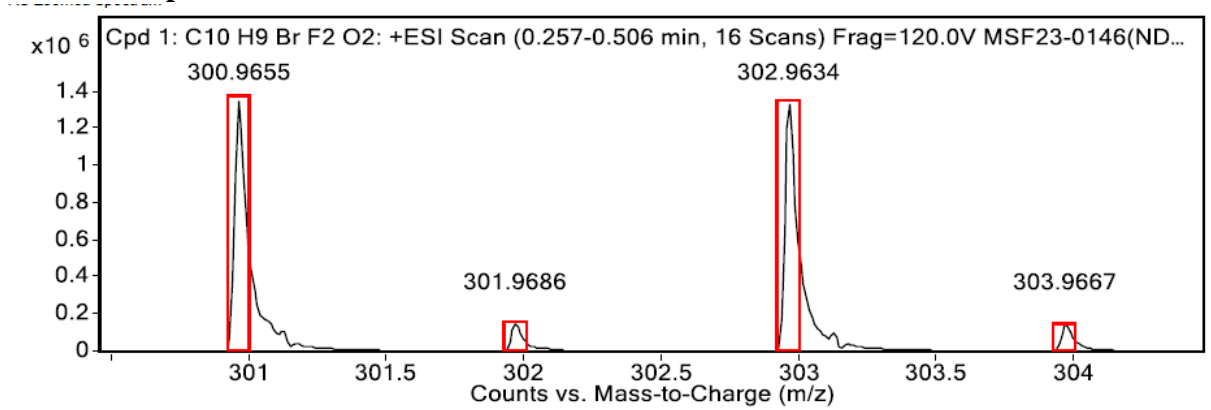

MS Spectrum Peak List

Obs. m/z	Calc. m/z	Charge	Abundance	Formula	Ion Species	Tgt Mass Error (ppm)
300.9655	300.9646	1	1367532	C10H9BrF2O2	(M+Na)+	-2.94
301.9686	301.9680	1	154732	C10H9BrF2O2	(M+Na)+	-1.99
302.9634	302.9626	1	1336978	C10H9BrF2O2	(M+Na)+	-2.46
303.9667	303.9660	1	153703	C10H9BrF2O2	(M+Na)+	-2.15
304.9635	304.9683	1	15319	C10H9BrF2O2	(M+Na)+	15.77

Figure S4.1. HRMS of **4-(3-bromopropoxy)-2,6-difluorobenaldehyde**

(ESI-TOF, pos. mode, acetonitrile)

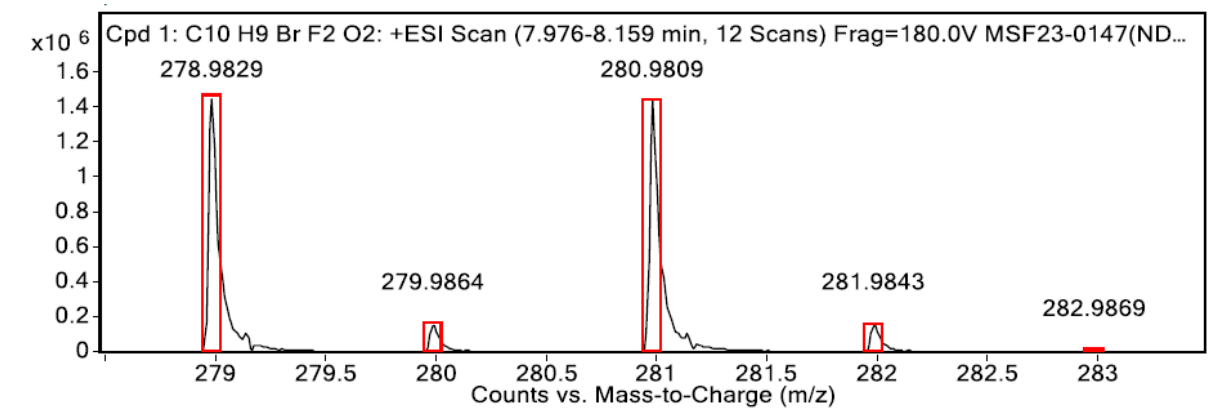

MS Spectrum Peak List

Obs. m/z	Calc. m/z	Charge	Abundance	Formula	Ion Species	Tgt Mass Error (ppm)
159.0248			2075440			
278.9829	278.9827	1	1455297	C10H9BrF2O2	(M+H)+	-0.67
279.9864	279.9861	1	163942	C10H9BrF2O2	(M+H)+	-1.09
280.9809	280.9807	1	1455934	C10H9BrF2O2	(M+H)+	-0.53
281.9843	281.9841	1	164632	C10H9BrF2O2	(M+H)+	-1

Figure S4.2. HRMS of **4-(3-bromopropoxy)-3,5-difluorobenaldehyde**

(ESI-TOF, pos. mode, acetonitrile)

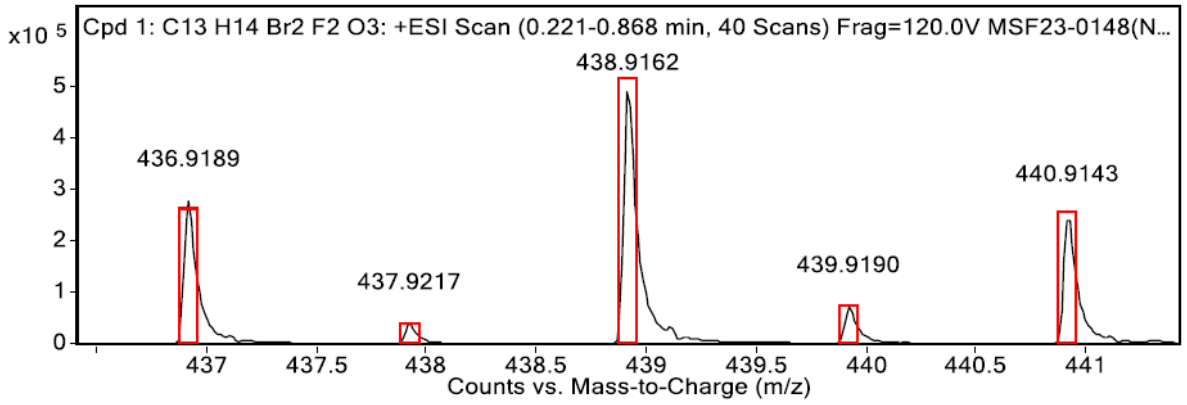

MS Spectrum Peak List

Obs. m/z	Calc. m/z	Charge	Abundance	Formula	Ion Species	Tgt Mass Error (ppm)
436.9189	436.9170	1	280144	C13H14Br2F2O3	(M+Na)+	-4.46
438.9162	438.9150	1	500503	C13H14Br2F2O3	(M+Na)+	-2.62
439.9190	439.9184	1	73814	C13H14Br2F2O3	(M+Na)+	-1.46
440.9143	440.9131	1	250873	C13H14Br2F2O3	(M+Na)+	-2.67
596.8723			565083			

Figure S4.3. HRMS of **3,5-bis(3-bromopropoxy)-2,6-difluorobenaldehyde**

(ESI-TOF, pos. mode, acetonitrile)

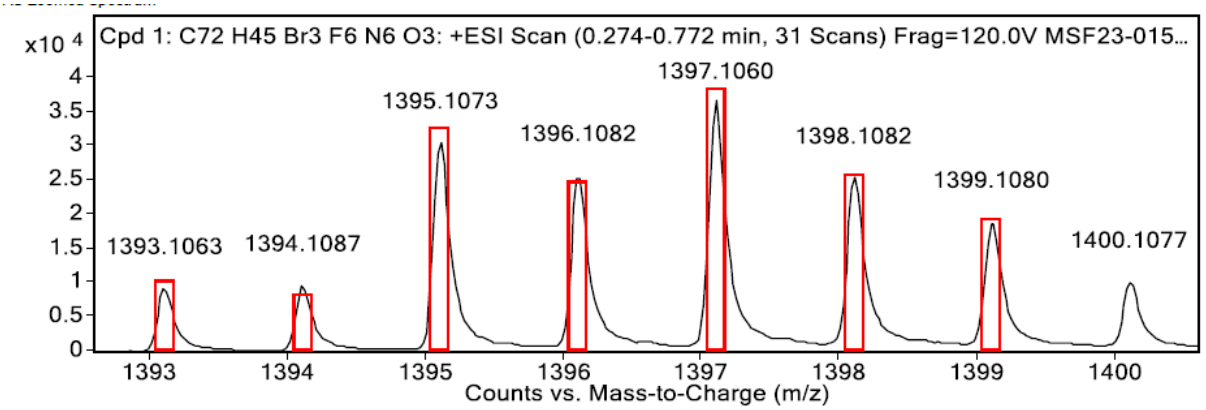

MS Spectrum Peak List

Obs. m/z	Calc. m/z	Charge	Abundance	Formula	Ion Species	Tgt Mass Error (ppm)
129.0518			72516			
1393.1063	1393.1080	1	9271	C72H45Br3F6N6O3	(M+H)+	1.23
1394.1087	1394.1112	1	9674	C72H45Br3F6N6O3	(M+H)+	1.8
1395.1073	1395.1068	1	30531	C72H45Br3F6N6O3	(M+H)+	-0.31
1396.1082	1396.1095	1	25773	C72H45Br3F6N6O3	(M+H)+	0.95
1397.1060	1397.1061	1	36732	C72H45Br3F6N6O3	(M+H)+	0.07
1398.1082	1398.1080	1	25414	C72H45Br3F6N6O3	(M+H)+	-0.15
1399.1080	1399.1065	1	18981	C72H45Br3F6N6O3	(M+H)+	-1.12
1400.1077	1400.1073	1	10200	C72H45Br3F6N6O3	(M+H)+	-0.23

Figure S4.4. HRMS of **NRos-4** (ESI-TOF, pos. mode, acetonitrile)

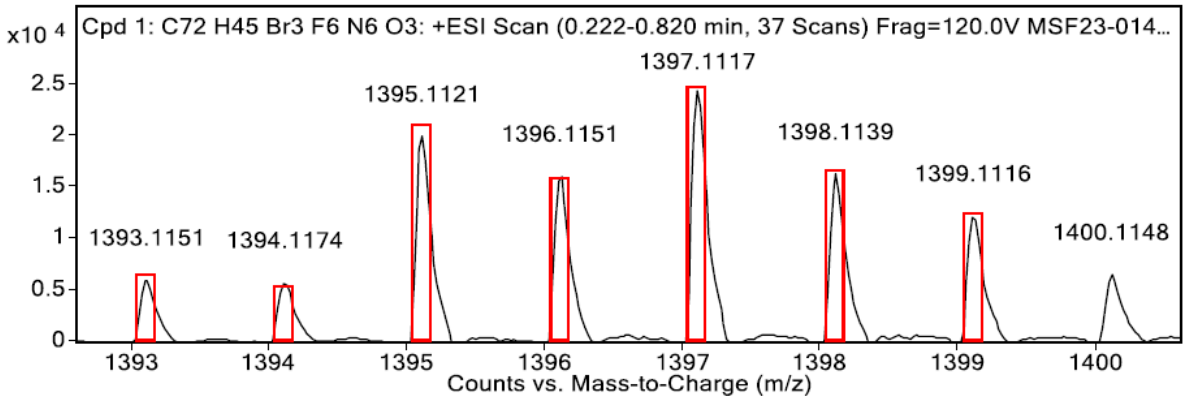

MS Spectrum Peak List

Obs. m/z	Calc. m/z	Charge	Abundance	Formula	Ion Species	Tgt Mass Error (ppm)
610.1843			50720			
1393.1151	1393.1080	1	6064	C72H45Br3F6N6O3	(M+H)+	-5.06
1394.1174	1394.1112	1	5815	C72H45Br3F6N6O3	(M+H)+	-4.46
1395.1121	1395.1068	1	20026	C72H45Br3F6N6O3	(M+H)+	-3.78
1396.1151	1396.1095	1	16162	C72H45Br3F6N6O3	(M+H)+	-4
1397.1117	1397.1061	1	24474	C72H45Br3F6N6O3	(M+H)+	-3.97
1398.1139	1398.1080	1	16365	C72H45Br3F6N6O3	(M+H)+	-4.24
1399.1116	1399.1065	1	12297	C72H45Br3F6N6O3	(M+H)+	-3.68
1400.1148	1400.1073	1	6593	C72H45Br3F6N6O3	(M+H)+	-5.32

Figure S4.5. HRMS of **NRos-5** (ESI-TOF, pos. mode, acetonitrile)

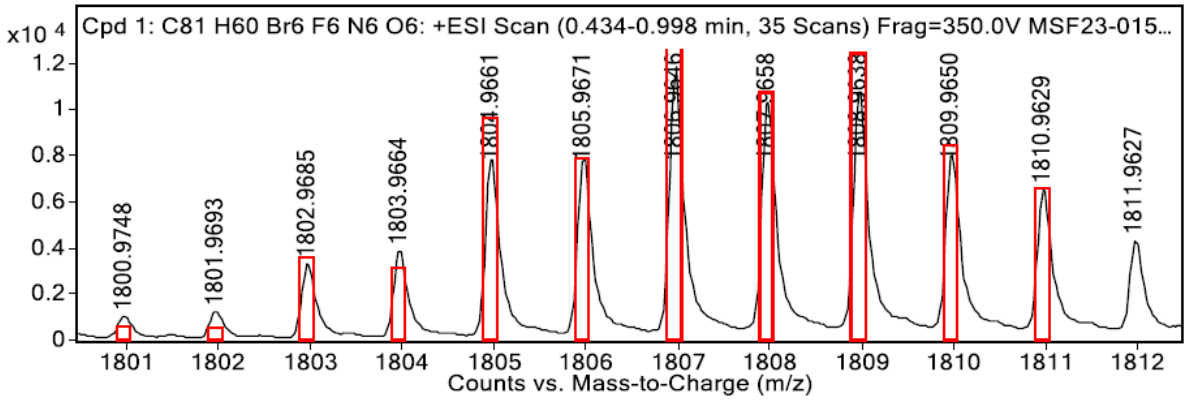

MS Spectrum Peak List

Obs. m/z	Calc. m/z	Charge	Abundance	Formula	Ion Species	Tgt Mass Error (ppm)
1788.9744			27497			
1800.9748	1800.9652	1	1123	C81H60Br6F6N6O6	(M+H)+	-5.33
1803.9664	1803.9665	1	3957	C81H60Br6F6N6O6	(M+H)+	0.1
1804.9661	1804.9623	1	8003	C81H60Br6F6N6O6	(M+H)+	-2.06
1805.9671	1805.9648	1	7977	C81H60Br6F6N6O6	(M+H)+	-1.3
1806.9646	1806.9612	1	11702	C81H60Br6F6N6O6	(M+H)+	-1.9
1807.9658	1807.9631	1	10452	C81H60Br6F6N6O6	(M+H)+	-1.51
1808.9638	1808.9603	1	10970	C81H60Br6F6N6O6	(M+H)+	-1.94
1809.9650	1809.9617	1	8155	C81H60Br6F6N6O6	(M+H)+	-1.82
1810.9629	1810.9599	1	6619	C81H60Br6F6N6O6	(M+H)+	-1.64
1811.9627	1811.9606	1	4408	C81H60Br6F6N6O6	(M+H)+	-1.11

Figure S4.6. HRMS of **NRos-6** (ESI-TOF, pos. mode, acetonitrile)

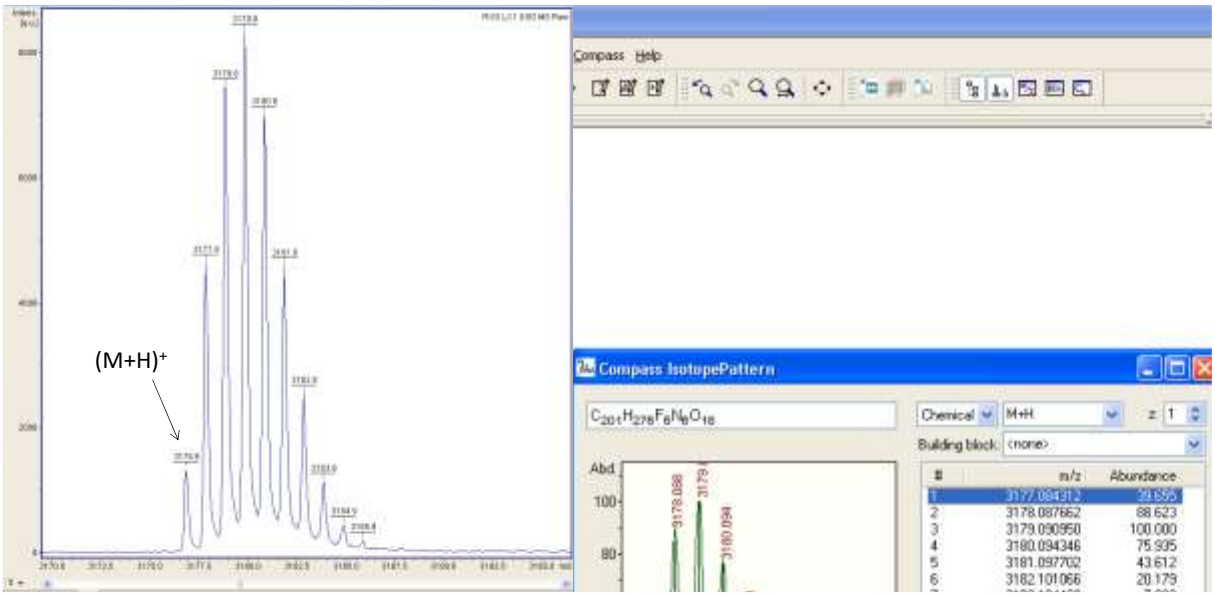

Figure S4.7. MALDI-TOF mass spectrum of **NRos-1.**

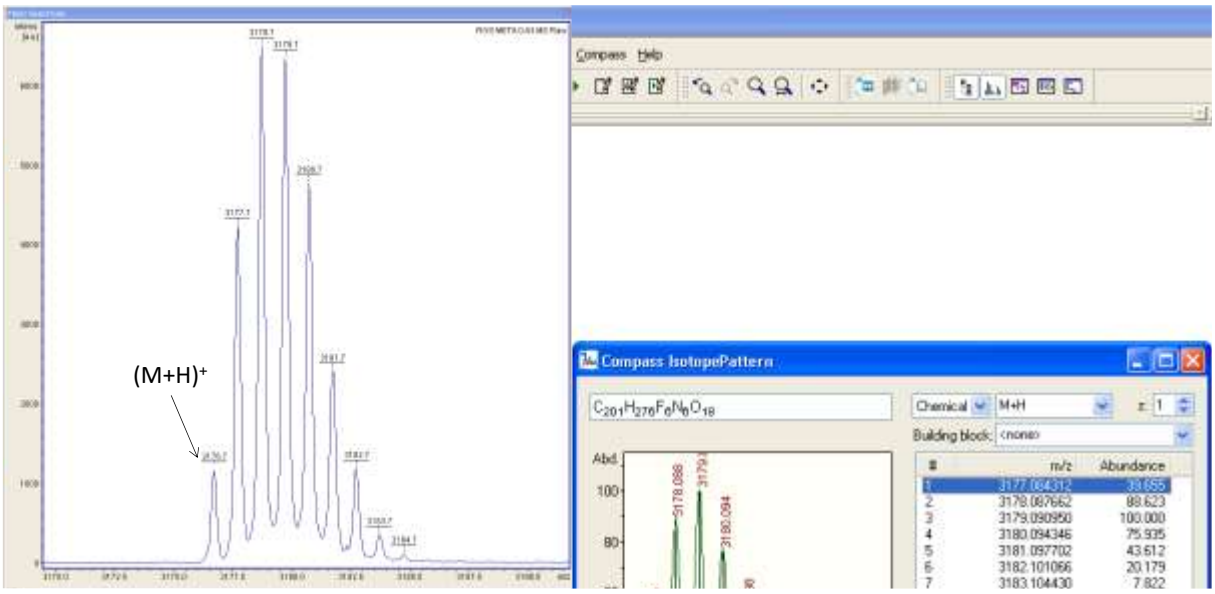

Figure S4.8. MALDI-TOF mass spectrum of **NRos-2**

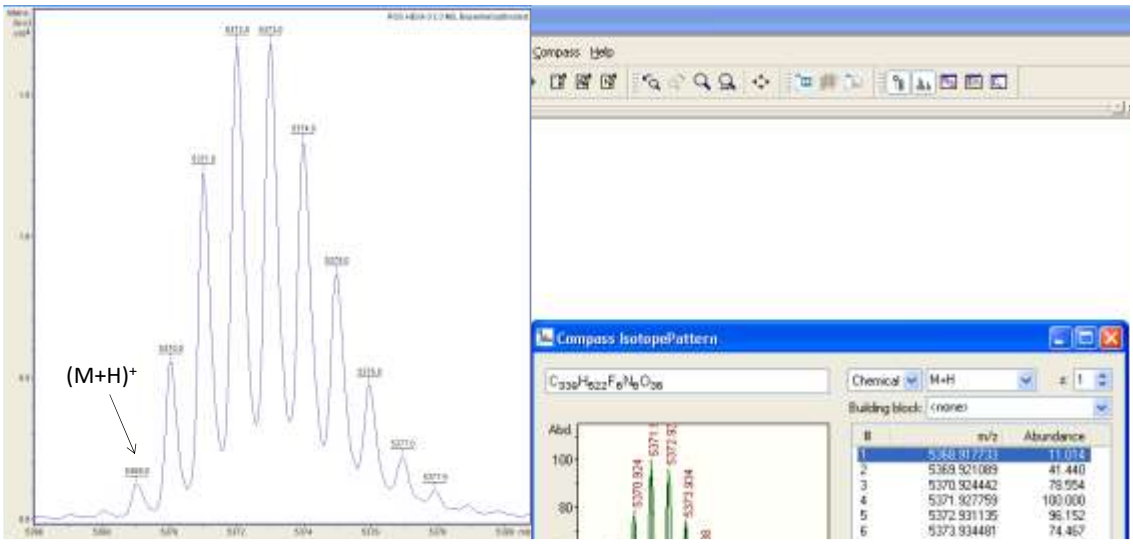

Figure S4.9. MALDI-TOF mass spectrum of **NRos-3**

5. UV-Vis spectra

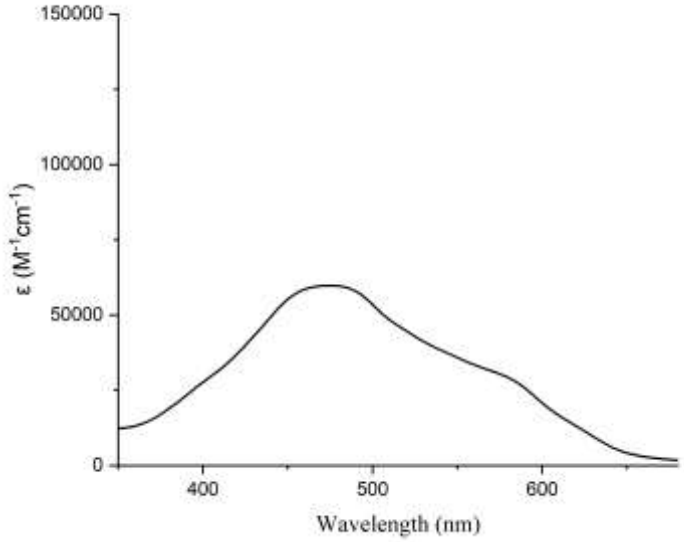

Figure S5.1. UV/Vis absorption spectrum of **NRos-4**

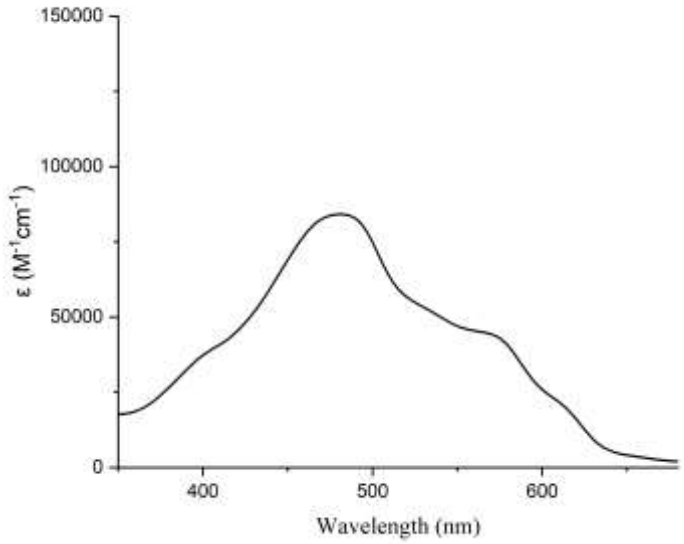

Figure S5.2. UV/Vis absorption spectrum of of **NRos-5**

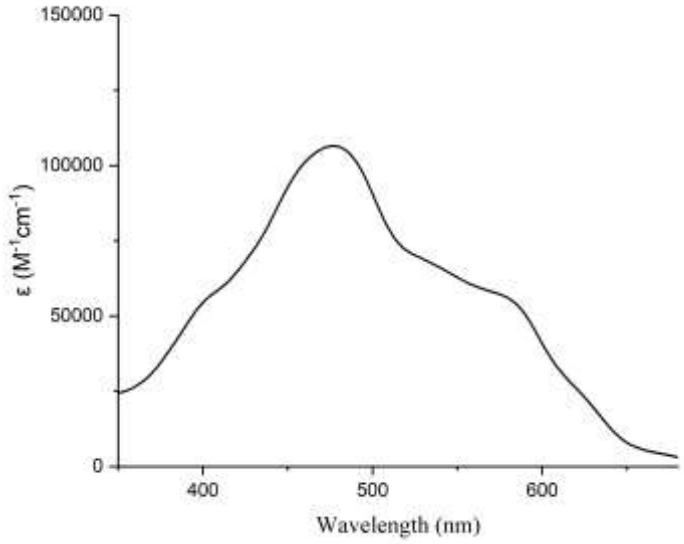

Figure S5.3. UV/Vis absorption spectrum of of **NRos-6**

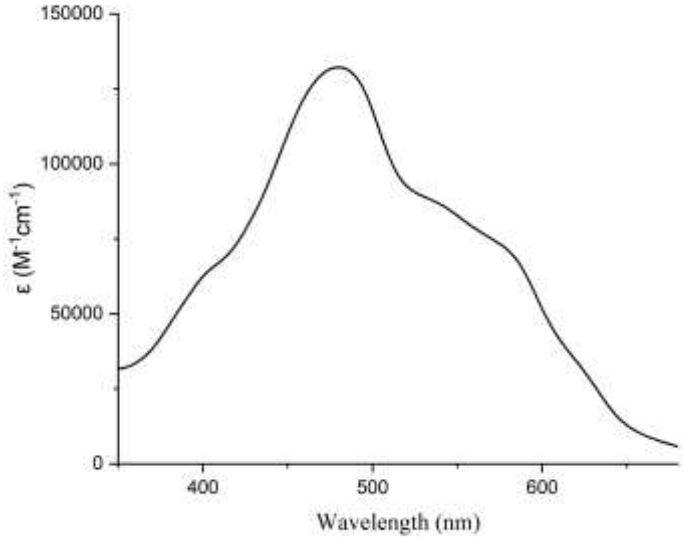

Figure S5.4. UV/Vis absorption spectrum of **NRos-1**

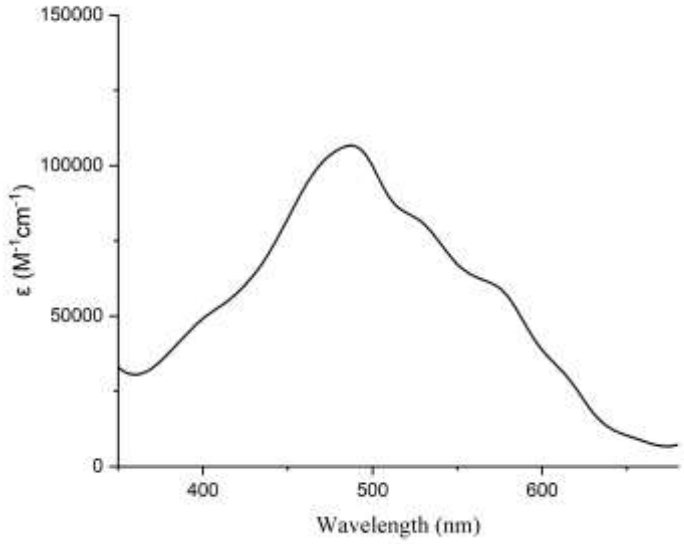

Figure S5.5. UV/Vis absorption spectrum of **NRos-2**

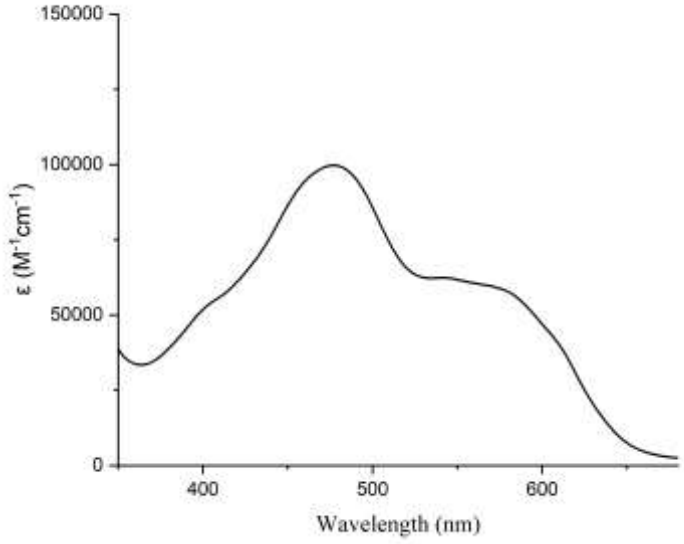

Figure S5.6. UV/Vis absorption spectrum of **NRos-3**

6. Computational Studies

All reported structures were optimized at the GFN2-xTB level[3] in the gas phase. Dimeric structures were also optimized by DFT to assess the discrepancies with the above-mentioned method. The DFT calculations were conducted using the B3LYP functional[4] and the standard 6-31G(d) basis set. All of the calculations were carried out using the methods implemented in the Gaussian 16 package.[5] As the DFT calculations proved concordant with those optimized at

the GFN2-xTB level similar results, we decided to complete the study with GFN2-xTB in order to reduce computational costs.

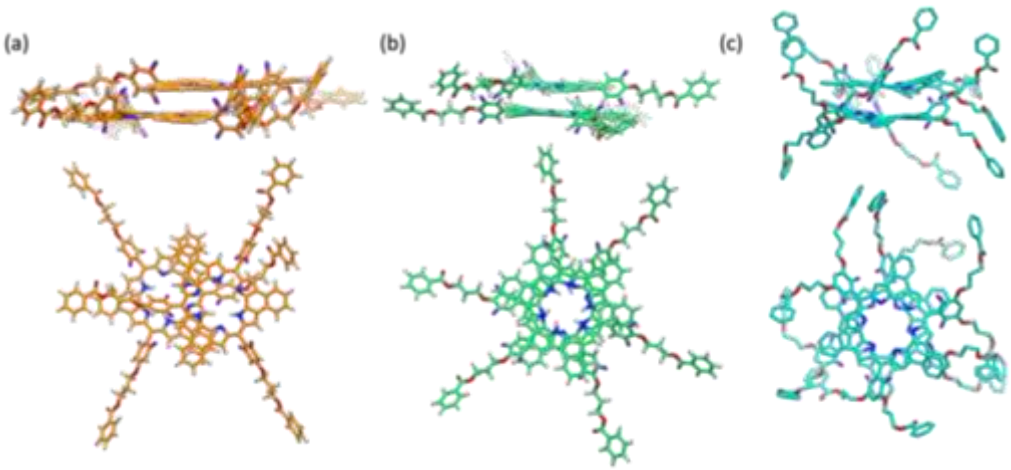

Figure S6.1. Top and side views of the supramolecular dimers of (a) **NRos-1**, (b) **NRos-2** and (c) **NRos-3** fully optimized at the GFN2-xTB level. Carbons atoms of **NRos-1**, **NRos-2** and **NRos-3** are represented in orange, green and blue, respectively.

7. Differential scanning calorimetry

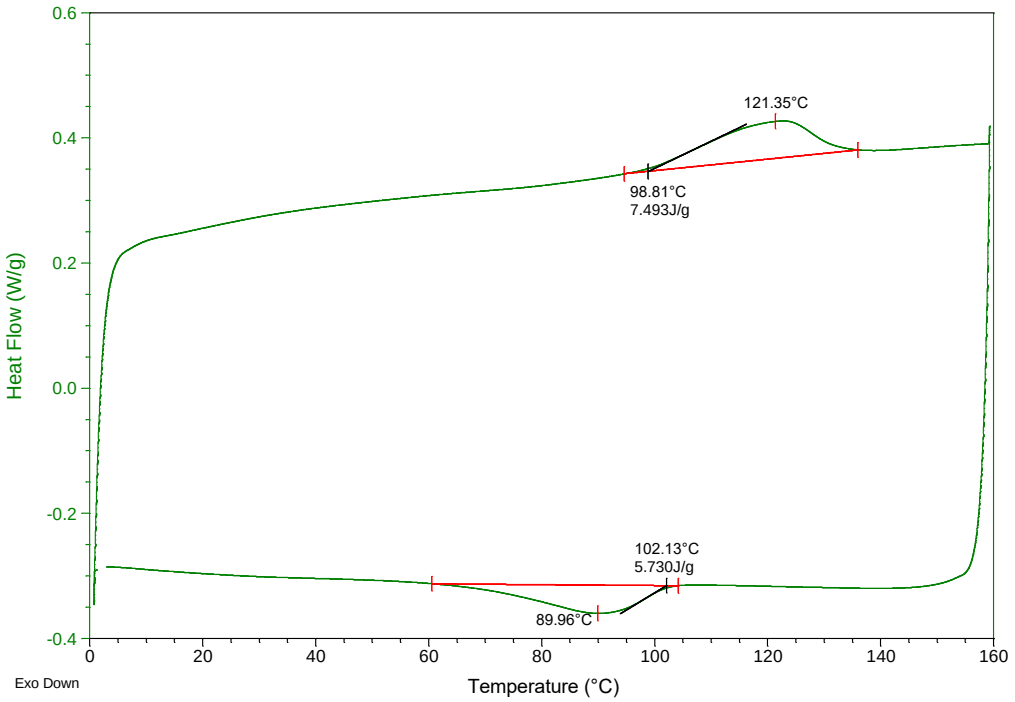

Figure S7.1. Second heating-cooling cycle thermogram of **NRos-1** recorded at a rate of 10 ºC/min (thermogravimetric analysis: 215 °C 3.000% weight loss).

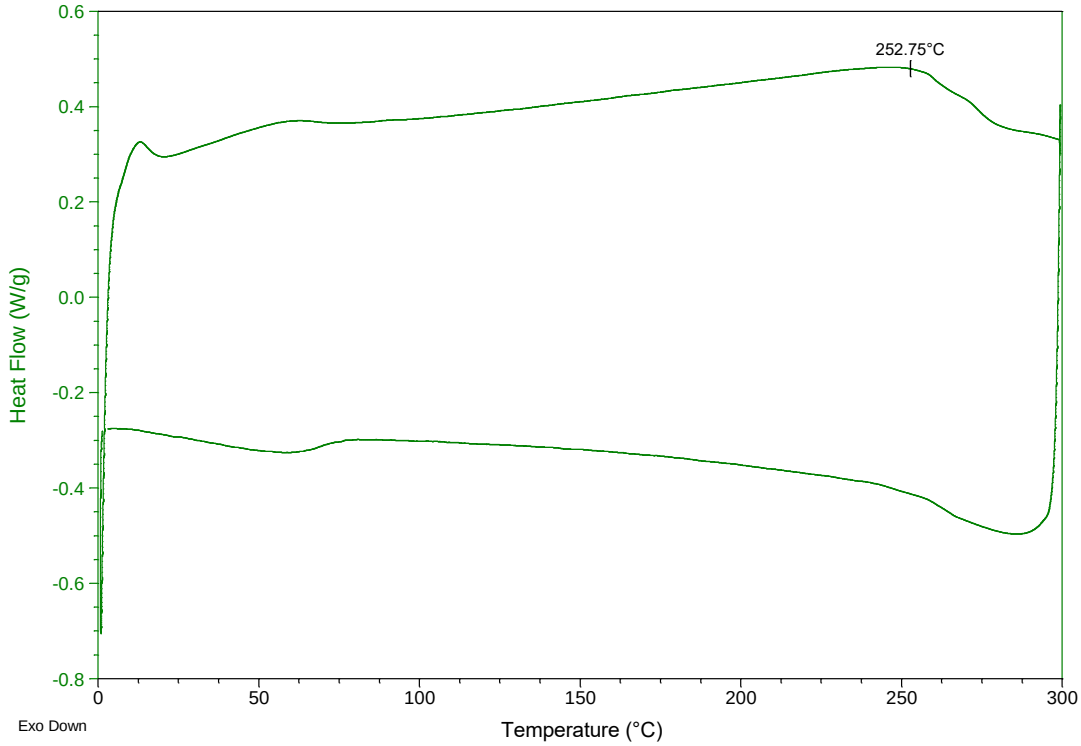

Figure S7.2. Second heating-cooling cycle thermogram of **NRos-2** recorded at a rate of 10 ºC/min (thermogravimetric analysis: 333.3 °C 3.000% weight loss).

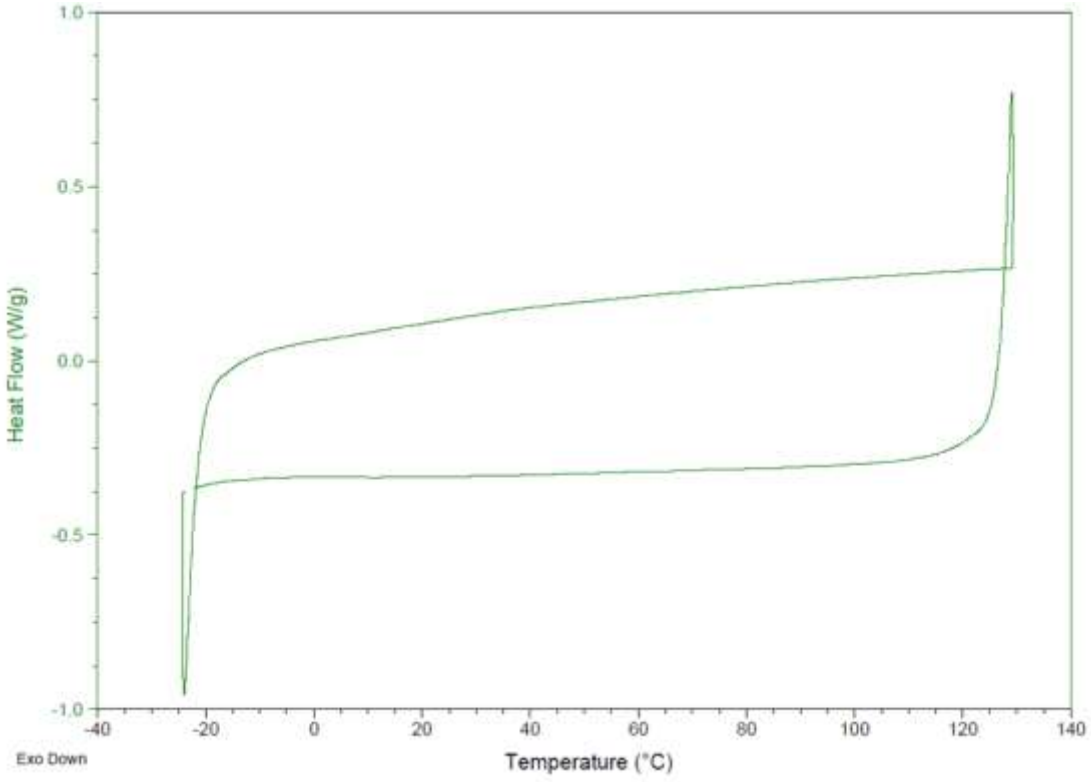

Figure S7.3. Heating-cooling cycle thermogram of **NRos-3** recorded at a rate of 10 ºC/min (thermogravimetric analysis: 157.6 °C 3.000% weight loss).

8. X-ray diffraction

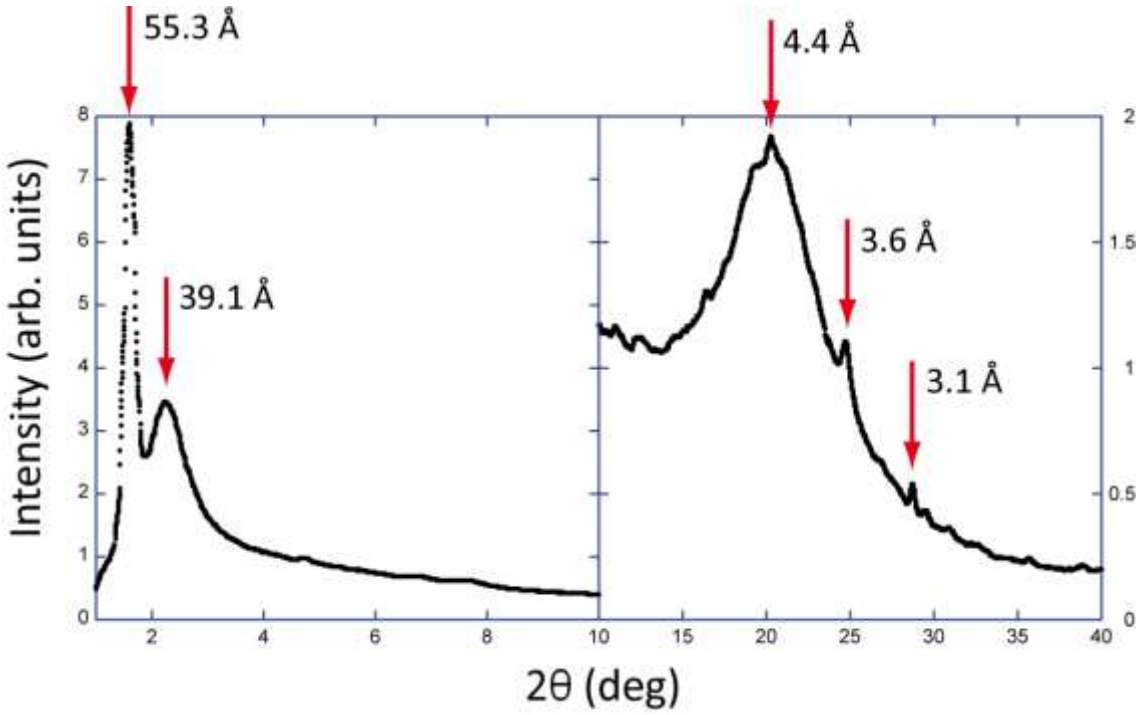

Figure S8.1. X-ray diffraction diagram of **NRos-1** at room temperature. The angle region for $2\theta \geq 10°$ was enlarged for clarity. Some spaces are indicated.

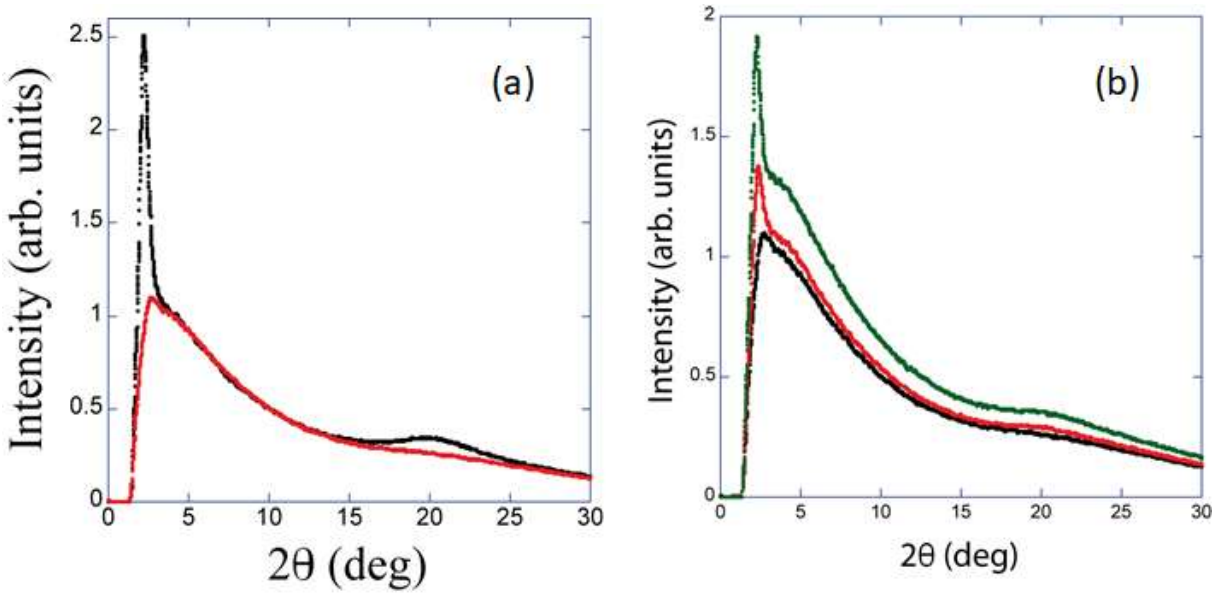

Figure S8.2: X-ray diffractions diagrams of **NRos-3**: (a) recorded at room temperature (black) and at 125 °C, in the isotropic liquid state; and (b) recorded on cooling from the isotropic liquid (125 °C, black) to room temperature (red: immediately upon cooling, green: after about 20 h).

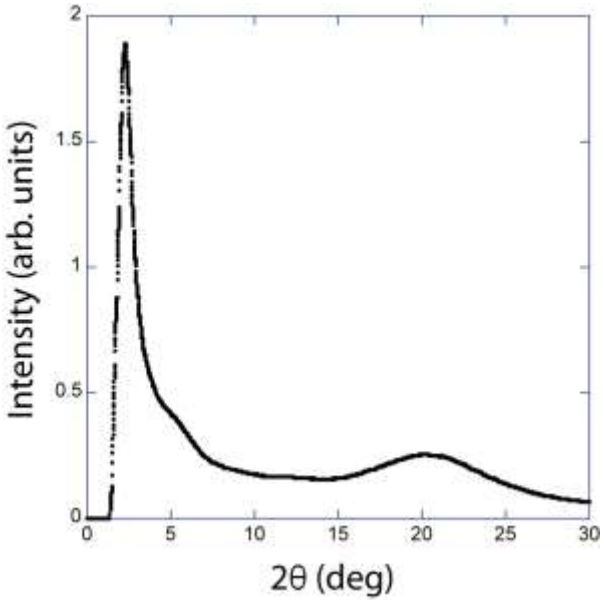

Figure S8.3: X-ray diffraction diagram of **NRos-2** recorded at room temperature.

9. Polarized optical microscopy

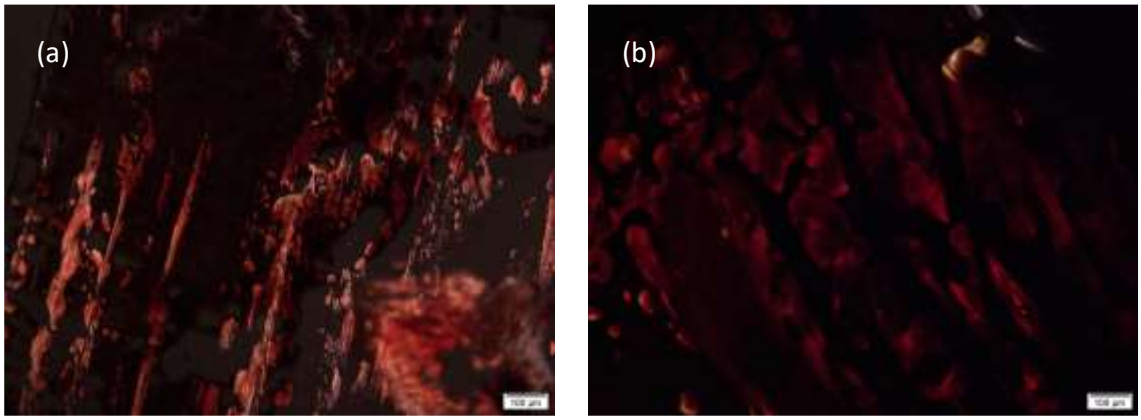

Figure S9.1. POM images taken after mechanical shearing of (a) **NRos-2** at 95 °C, and (b) **NRos-3** at 100 °C.

10. Supporting References

[1] N. R. Babij, E. O. McCusker, G. T. Whiteker, B. Canturk, N. Choy, L. C. Creemer, C. V. D. Amicis, N. M. Hewlett, P. L. Johnson, J. A. Knobelsdorf, F. Li, B. A. Lorsbach, B. M. Nugent, S. J. Ryan, M. R. Smith and Q. Yang, *Org. Process Res. Dev*. 2016, **20**, 661.

[2] Roznyatovskiy, V., Lynch, V. and Sessler, J. L., *Org. Lett*, 2010, **12**, 4424–4427.

[3] C. Bannwarth, S. Ehlert, S. Grimme, *J. Chem. Theory Comput.* 2019, **15**, 1652–1671

[4] (a) C. Lee, W. Yang, R. G. Parr, *Phys. Rev. B* 1988, **37**, 785–789. (b) A. D. Becke, *J. Chem. Phys.* 1993, **98**, 5648. (c) W. Kohn, A. D. Becke, R. G. Parr, *J. Phys. Chem.* 1996, **100**, 12974–12980

[5] Gaussian 16, Revision C.01; Frisch, M. J.; Trucks, G. W.; Schlegel, H. B.; Scuseria, G. E.; Robb, M. A.; Cheeseman, J. R.; Scalmani, G.; Barone, V.; Petersson, G. A.; Nakatsuji, H.; Li, X.; Caricato, M.; Marenich, A. V.; Bloino, J.; Janesko, B. G.; Gomperts, R.; Mennucci, B.; Hratchian, H. P.; Ortiz, J. V.; Izmaylov, A. F.; Sonnenberg, J. L.; Williams-Young, D.; Ding, F.; Lipparini, F.; Egidi, F.; Goings, J.; Peng, B.; Petrone, A.; Henderson, T.; Ranasinghe, D.; Zakrzewski, V. G.; Gao, J.; Rega, N.; Zheng, G.; Liang, W.; Hada, M.; Ehara, M.; Toyota, K.; Fukuda, R.; Hasegawa, J.; Ishida, M.; Nakajima, T.; Honda, Y.; Kitao, O.; Nakai, H.; Vreven, T.; Throssell, K.; Montgomery, J. A., Jr.; Peralta, J. E.; Ogliaro, F.;

Bearpark, M. J.; Heyd, J. J.; Brothers, E. N.; Kudin, K. N.; Staroverov, V. N.; Keith, T. A.; Kobayashi, R.; Normand, J.; Raghavachari, K.; Rendell, A. P.; Burant, J. C.; Iyengar, S. S.; Tomasi, J.; Cossi, M.; Millam, J. M.; Klene, M.; Adamo, C.; Cammi, R.; Ochterski, J. W.; Martin, R. L.; Morokuma, K.; Farkas, O.; Foresman, J. B.; Fox, D. J. Gaussian, Inc., Wallingford CT, 2016